Published for SISSA by Springer

Received: *July 31, 2012*
Accepted: *October 15, 2012*
Published: *November 5, 2012*

Holography, chiral Lagrangian and form factor relations

Pietro Colangelo, Juan Jose Sanz-Cillero and Fen Zuo

Istituto Nazionale di Fisica Nucleare, Sezione di Bari,
Via E. Orabona 4, I-70125 Bari, Italy

E-mail: Pietro.Colangelo@ba.infn.it, Juan.SanzCillero@ba.infn.it, fen.zuo@ba.infn.it

Abstract: We derive all the $\mathcal{O}(p^6)$ Chiral Perturbation Theory low-energy constants from a class of gravity dual models of QCD described by the Yang-Mills and Chern-Simons Lagrangian terms, with the chiral symmetry broken through boundary conditions in the infrared. All the constants of the odd intrinsic parity sector are universally determined by those at $\mathcal{O}(p^4)$ in the even sector, together with an extra resonance term. A few relations for the even sector couplings are also extracted. Our estimates reasonably agree with the few available $\mathcal{O}(p^6)$ determinations from alternative phenomenological analyses. Some of the relations between low-energy constants are the manifestation, at large distances, of universal relations that we find between form factors in the even and odd sectors, e.g., between the $\gamma^* \to \pi\pi$ and $\pi \to \gamma\gamma^*$ matrix elements.

Keywords: AdS-CFT Correspondence, 1/N Expansion, Chiral Lagrangians, QCD

ArXiv ePrint: 1207.5744

doi:10.1007/JHEP11(2012)012

JHEP11(2012)012

Contents

1 Introduction

Chiral symmetry is a crucial ingredient for the understanding of the light quark interactions. The low-energy dynamics of the pseudo-Goldstone bosons from the spontaneous symmetry breaking is provided by the corresponding effective field theory (EFT), Chiral Perturbation Theory (χPT), with a perturbative expansion in powers of light quark masses and external momenta [1–4]. This allows a systematic description of the long-distance

JHEP11(2012)012

regime of QCD, at energies below the lightest resonance mass. The precision required in present phenomenological applications makes necessary to include corrections of $\mathcal{O}(p^6)$. While many two-loop χPT calculations have been already carried out [5, 6], the large number of unknown low-energy constants (LECs) appearing at this order puts a limit to the achievable accuracy. The determination of these χPT couplings is compulsory to further progress in our understanding of strong interactions at low energies. Various techniques have allowed the determination of some $\mathcal{O}(p^6)$ LECs: direct comparison of next-to-next-leading order (NNLO) χPT computations and experiment [7, 8], sum rules and dispersion relations [9–11], Padé approximants [12–14], resonance chiral Lagrangians [15, 16], Dyson-Schwinger equation (DSE) [17, 18].

In this paper we study the LECs in a class of holographic theories, which was first proposed in ref. [19], based on early ideas of dimensional deconstruction [20, 21] and hidden local symmetry [22]. Later, an explicit model of this kind was constructed from string theory , in which chiral symmetry breaking was implemented geometrically through the embedding of the flavor branes [23]. At the same time, it was realized that chiral symmetry breaking can actually be induced by different boundary conditions (b.c.) in the infrared [24]. In this kind of models, the chiral Lagrangian up to order p^4 is automatically accommodated, both of the even intrinsic parity sector [24] and of the odd sector [23, 25]. Moreover, the predictions for $\mathcal{O}(p^4)$ LECs have slight model dependence [24, 26], and agree quite well with the experimental data. This success at $\mathcal{O}(p^4)$ has motivated the present study of the $\mathcal{O}(p^6)$ LECs within the same class of models. There are also other holographic calculations of the LECs [27] in another framework involving the quark condensate [27, 28].

The other motivation for our study is that this kind of models have recently led to an interesting relation between the left-right quark current correlator $\Pi_{LR}(Q^2)$ and the transverse part $w_T(Q^2)$ of the anomalous AVV Green's function, the so-called Son-Yamamoto relation [29]. The relation does not depend on the details of the different models among this class, showing some kind of universality. When extrapolated to the large momentum region and combined with the results of the operator product expansion in QCD, the relation gives the same prediction of the magnetic susceptibility as the early prediction by Vainshtein [30]. However, while the power correction on the $\Pi_{LR}(Q^2)$ side can be included [29, 31, 32] through the dual scalar field of the quark condensate [27, 28], the holographic description of the power corrections in $w_T(Q^2)$ is still unclear, making the naive extrapolation ambiguous. For recent studies along this line, see [33–36].

The corresponding analysis at low energies yields a relation between the $\mathcal{O}(p^4)$ even-parity χPT coupling L_{10} and the $\mathcal{O}(p^6)$ odd-intrinsic-parity coupling C_{22}^W which, respectively, rule the left-right and AVV Green's functions at large distances [37, 38]. Numerically this relation is reasonably well satisfied at low energies [31]. Through a detailed analysis of the $\mathcal{O}(p^6)$ predictions for the LECs of the odd-intrinsic parity sector in this kind of models, we find further relations between the remaining LECs C_j^W and the $\mathcal{O}(p^4)$ chiral couplings from the even-parity sector. A few relations among the $\mathcal{O}(p^6)$ LECs in the even sector have also been found.

At this stage, one may wonder whether these relations between even and odd sector LECs hint a more general interplay between even-parity and anomalous QCD amplitudes.

JHEP11(2012)012

Here we have focused on the odd couplings C_{22}^W and C_{23}^W, which can be directly related to the transition of a pion into two photons and two axial-vector currents, respectively. We shall show that the former amplitude can be related to the vector form factor of the pion and the latter to the axial-vector form factor into three pions [39, 40]. The relation involving the vector form factor has already been found in two specific models [41, 42].

In section 2 we provide the details of the class of holographic models employed in our analysis, and review the previous results for the $\mathcal{O}(p^2)$ and $\mathcal{O}(p^4)$ LECs. In section 3 the NNLO LECs are computed, with the help of a series of novel sum rules involving the resonance couplings. In addition, we shall check how well these sum rules are saturated by the lightest resonances. We also point out that possible corrections to the LECs could come from higher dimensional terms, which will appear in the α' expansion in the dual string theory, and also from scalar resonances not included in the formalism. The two relations between the the form factors of the pion in the even and odd sector are derived in section 4. Our conclusions are gathered in section 5. Some technical details about the different holographic models are collected in appendix A. In appendix B we study the proposal in ref. [36] that the Son-Yamamoto relation could hold at the loop level: we show that the amplitudes in general do not match beyond tree-level.

2 The holographic model

2.1 The 5D action

In the kind of models studied in this paper, with the chiral symmetry broken through b.c.'s, the action is composed by the Yang-Mills (YM) and Chern-Simons (CS) terms, describing the even and anomalous QCD sectors, respectively [19, 23–25]:

$$S = S_{\rm YM} + S_{\rm CS} \tag{2.1}$$

$$S_{\rm YM} = -\int d^5x \,{\rm tr}\left[-f^2(z)\mathcal{F}_{z\mu}^2 + \frac{1}{2g^2(z)}\mathcal{F}_{\mu\nu}^2\right], \tag{2.2}$$

$$S_{\rm CS} = -\kappa\int {\rm tr}\left[\mathcal{A}\mathcal{F}^2 + \frac{i}{2}\mathcal{A}^3\mathcal{F} - \frac{1}{10}\mathcal{A}^5\right]. \tag{2.3}$$

The fifth coordinate z runs from $-z_0$ to z_0 with $0 < z_0 \leq +\infty$. $\mathcal{A}(x,z) = \mathcal{A}_M dx^M$ is the 5D U(N_f) gauge field and $\mathcal{F} = d\mathcal{A} - i\mathcal{A}\wedge\mathcal{A}$ is the field strength. They are decomposed as $\mathcal{A} = \mathcal{A}^a t^a$ and $\mathcal{F} = \mathcal{F}^a t^a$, with the normalization of the generators ${\rm Tr}\{t^a t^b\} = \delta^{ab}/2$. The coefficient $\kappa = N_C/(24\pi^2)$, with N_C the number of colors, is fixed by the chiral anomaly of QCD [43–45]. The functions $f^2(z)$ and $g^2(z)$ are invariant under the reflection $z \to -z$ so that parity can be properly defined in the model. In appendix A we provide their explicit definitions for the models we analyze here: flat metric [19], "Cosh" model [19], hard wall [24] and the Sakai-Sugimoto (SS) model [23, 25].

As first shown in ref. [19], chiral symmetry can be realized as a 5D gauge symmetry localized on the two boundaries at $z = \pm z_0$. The gauging of the chiral symmetry allows one to naturally introduce the corresponding right and left current sources, respectively $r_\mu(x)$ and $\ell_\mu(x)$. The Goldstone bosons are contained in the gauge component $\mathcal{A}_z$ and can be

JHEP11(2012)012

parameterized through the chiral field U as

$$\mathrm{U}(x^\mu) = \mathrm{P}\exp\left\{i\int_{-z_0}^{+z_0}\mathcal{A}_z(x^\mu,z')dz'\right\}, \tag{2.4}$$

which transforms as

$$\mathrm{U}(x) \to g_R(x)\mathrm{U}(x)g_L^\dagger(x) \tag{2.5}$$

with $g_L(x)$ and $g_R(x)$ the gauge transformations located at $z=-z_0$ and $z=z_0$, respectively. The vector/axial-vector resonances are contained in the gauge field components $\mathcal{A}_\mu$,

$$\mathcal{A}_\mu(x,z) = \ell_\mu(x)\psi_-(z) + r_\mu(x)\psi_+(z) + \sum_{n=1}^{\infty} B_\mu^{(n)}(x)\psi_n(z)\,, \tag{2.6}$$

with the UV boundary conditions

$$\mathcal{A}_\mu(x,-z_0) = \ell_\mu(x)\,, \qquad\qquad \mathcal{A}_\mu(x,z_0) = r_\mu(x)\,. \tag{2.7}$$

Note that the above boundary conditions are different from those in refs. [25, 29], and correspondingly the sign of the CS action is different.

The resonance wave-functions $\psi_n(z)$ are provided by the normalizable eigenfunctions of the equation of motion for the transverse part of the gauge field,

$$-\,g^2(z)\,\partial_z[f^2(z)\partial_z\mathcal{A}_\mu(q,z)] \;=\; q^2\mathcal{A}_\mu(q,z)\,, \tag{2.8}$$

with the resonance masses given by the eigenvalues $q^2 = m_n^2$, with b.c.'s $\psi_n(\pm z_0) = 0$. The 4D metric signature $(+,-,-,-)$ is assumed all along the article. In order to have canonically normalized kinetic terms for the resonance fields in the later derivation, the orthogonal wave-functions are chosen to be normalized in the form

$$\int_{-z_0}^{+z_0}\frac{1}{g^2(z)}\psi_n(z)\psi_m(z)\;\mathrm{d}z = \delta_{nm}\,, \tag{2.9}$$

leading to the completeness condition,

$$\sum_{n=1}^{\infty}\frac{1}{g^2(z)}\psi_n(z)\psi_n(z') = \delta(z-z')\,. \tag{2.10}$$

In addition, one has $\psi_\pm(z) = \frac{1}{2}(1\pm\psi_0(z))$, where $\psi_0(z)$ is the solution of the EoM at $q^2=0$ with b.c.'s $\psi_0(\pm z_0) = \pm 1$. It is non-normalizable and will provide the chiral Goldstone wave-function.

The solutions $\psi_n(z)$ are even (odd) functions of z when n is odd (even). Thus, the modes with odd n describe vector excitations $v_\mu^n = B_\mu^{(2n-1)}$ with $m_{v^n}^2 = m_{2n-1}^2$, and those with even n correspond to axial-vector resonances in an analogous way.

We consider the convenient 5D gauge $\mathcal{A}_z = 0$, which can be achieved through the transformation $\mathcal{A}_M \to g\mathcal{A}_M g^{-1} + ig\partial_M g^{-1}$ with

$$g^{-1}(x,z) = P\exp\left\{i\int_0^z dz'\,\mathcal{A}_z(x,z')\right\}\,. \tag{2.11}$$

JHEP11(2012)012

The value of this transformation on the UV branes is given by $\xi_{R(L)}(x) \equiv g^{-1}(x, \pm z_0)$, which now encode the original information from $\mathcal{A}_z$. The chiral Goldstones can be then non-linearly realized through the coset representative $\xi_R(x) = \xi_L(x)^\dagger \equiv u(\pi) = \exp\{i\pi^a t^a/f_\pi\}$ [5, 6, 15, 16]. Conversely, after the gauge transformation the space-time components of the 5D field in eq. (2.6) takes the form

$$\mathcal{A}_\mu(x,z) = i\Gamma_\mu(x) + \frac{u_\mu(x)}{2}\psi_0(z) + \sum_{n=1}^{\infty} v_\mu^n(x)\psi_{2n-1}(z) + \sum_{n=1}^{\infty} a_\mu^n(x)\psi_{2n}(z)\,, \tag{2.12}$$

where the commonly used tensors from χPT [5, 6, 15, 16], $u_\mu(x)$ and $\Gamma_\mu(x)$, show up naturally:

$$u_\mu(x) \equiv \mathrm{i}\left\{\xi_R^\dagger(x)\left(\partial_\mu - \mathrm{i}r_\mu\right)\xi_R(x) - \xi_L^\dagger(x)\left(\partial_\mu - \mathrm{i}\ell_\mu\right)\xi_L(x)\right\} \tag{2.13}$$

$$\Gamma_\mu(x) \equiv \frac{1}{2}\left\{\xi_R^\dagger(x)\left(\partial_\mu - \mathrm{i}r_\mu\right)\xi_R(x) + \xi_L^\dagger(x)\left(\partial_\mu - \mathrm{i}\ell_\mu\right)\xi_L(x)\right\}. \tag{2.14}$$

Sometimes it is more convenient to work with the bulk-to-boundary propagators for the transverse part of the gauge field, rather than in the meson decomposition. These propagators are the solutions of eq. (2.8) for a general Euclidean squared momentum $Q^2 \equiv -q^2$, with b.c.'s $V(Q, \pm z_0) = 1$ and $A(Q, \pm z_0) = \pm 1$ ($Q = \sqrt{Q^2}$). They can be nonetheless expressed by means of the on-shell state decomposition in terms of the infinite summation

$$V(Q,z) = \sum_{n=1}^{\infty} \frac{g_{v^n}\psi_{2n-1}(z)}{Q^2 + m_{v^n}^2}\,, \qquad A(Q,z) = \sum_{n=1}^{\infty} \frac{g_{a^n}\psi_{2n}(z)}{Q^2 + m_{a^n}^2} \tag{2.15}$$

with the decay constants given as

$$g_{v^n} = -f^2(z)\partial_z\psi_{2n-1}(z)\,|_{-z_0}^{+z_0}\,, \qquad g_{a^n} = -f^2(z)\psi_0(z)\partial_z\psi_{2n}(z)\,|_{-z_0}^{+z_0}\,. \tag{2.16}$$

When Q^2 goes to 0, we have $V(Q,z) \to 1$ and $A(Q,z) \to \psi_0(z)$, which have been used before. Alternatively, one can use the Green function $G(Q^2; z, z')$, which satisfies the equation

$$g^2(z)\partial_z[f^2(z)\partial_z G(Q^2;z,z')] - Q^2 G(Q^2;z,z') = -g^2(z)\delta(z-z'), \tag{2.17}$$

together with the same UV boundary conditions as the ψ_n. With the completeness condition of the resonances, the Green function can be solved as

$$G(Q^2;z,z') = \sum_{n=1}^{\infty} \frac{\psi_n(z)\psi_n(z')}{Q^2 + m_n^2}. \tag{2.18}$$

Therefore, the bulk-to-boundary propagators defined above are related to the Green function as

$$\begin{aligned} V(Q,z) &= -f^2(z')\partial_{z'}G(Q^2;z,z')|_{z'=-z_0}^{z'=+z_0} \\ A(Q,z) &= -f^2(z')\psi_0(z')\partial_{z'}G(Q^2;z,z')|_{z'=-z_0}^{z'=+z_0}. \end{aligned} \tag{2.19}$$

JHEP11(2012)012

Contrarily, once the propagators are known the Green function can be immediately obtained:

$$G(Q^2,z,z') = \frac{1}{2W(Q^2)}\left[(V(Q,z)-A(Q,z))(V(Q,z')+A(Q,z'))\theta(z-z')\right.$$
$$\left.+\,(V(Q,z)+A(Q,z))(V(Q,z')-A(Q,z'))\theta(z'-z)\right]\,. \tag{2.20}$$

Here $W(Q^2)$ is the Wronskian of eq. (2.8)

$$W(Q^2) = f^2(z)[V(Q,z)\partial_z A(Q,z) - A(Q,z)\partial_z V(Q,z)], \tag{2.21}$$

which is independent of z. At zero momentum $W(0) = f_\pi^2/2$ and the Green function simplifies

$$G(0,z,z') = \frac{1}{f_\pi^2}\left[(1-\psi_0(z))(1+\psi_0(z'))\theta(z-z') + (1-\psi_0(z'))(1+\psi_0(z))\theta(z'-z)\right]\,. \tag{2.22}$$

2.2 The chiral couplings at $\mathcal{O}(p^2)$ and $\mathcal{O}(p^4)$

Once we have rewritten the 5D fields in terms of the chiral Goldstones and vector and axial-vector resonances, the derivation of the meson Lagrangian is rather straightforward. We consider the 5D gauge $\mathcal{A}_z = 0$ and substitute the $\mathcal{A}_\mu$ decomposition provided in eq. (2.12) in the 5D action (2.1). The Lagrangian is now expressed in terms of meson fields ($\xi_{R,L}(x)$,$v_\mu^n(x)$, $a_\mu^n(x)$) and the left and right current sources ($r_\mu(x)$, $\ell_\mu(x)$). Each of these terms of the action shows then a factorization into an integration over the fifth dimension, which provides the meson coupling, and an integration over the space-time components, which provides the chiral structure of the operator in the effective 4D action.

Hence, after substituting the $\mathcal{A}_\mu$ decomposition (2.12) in the YM action, one gets the even-parity action without resonance fields [23, 24]:

$$\begin{aligned} S_2[\pi]+S_4[\pi] = \int d^4x \Bigg[& \frac{f_\pi^2}{4} < u_\mu u^\mu > \\ & + L_1 < u_\mu u^\mu >^2 + L_2 < u_\mu u_\nu >< u^\mu u^\nu > + L_3 < u_\mu u^\mu u_\nu u_\nu > \\ & - iL_9 < f_{+\mu\nu} u^\mu u^\nu > + \frac{L_{10}}{4} < f_{+\mu\nu} f_+^{\mu\nu} - f_{-\mu\nu} f_-^{\mu\nu} > \\ & + \frac{H_1}{2} < f_{+\mu\nu} f_+^{\mu\nu} + f_{-\mu\nu} f_-^{\mu\nu} > \Bigg], \end{aligned} \tag{2.23}$$

with the covariant tensors $f_\pm^{\mu\nu} \equiv \xi_L^{-1}\ell^{\mu\nu}\xi_L \pm \xi_R^{-1} r^{\mu\nu}\xi_R$ containing the field-strengths $\ell^{\mu\nu}$ and $r^{\mu\nu}$ of the left and right sources respectively. At low energies these terms provide the Goldstone interaction at the dominant orders and produce the $\mathcal{O}(p^2)$ and $\mathcal{O}(p^4)$ χPT

JHEP11(2012)012

	flat [19]	Cosh [19]	hard-wall [24]	Sakai-Sugimoto [23, 25]	χPT [2–4]
$10^3\ L_1$	0.5	0.5	0.5	0.5	0.9 ± 0.3
$10^3\ L_2$	1.0	1.0	1.0	1.0	1.7 ± 0.7
$10^3\ L_3$	-3.1	-3.2	-3.1	-3.1	-4.4 ± 2.5
$10^3\ L_9$	5.2	6.3	6.8	7.7	7.4 ± 0.7
$10^3\ L_{10}$	-5.2	-6.3	-6.8	-7.7	-6.0 ± 0.7
$10^3\ Y$	0.5	0.5	0.5	0.6	—
$10^3\ Z$	0.6	0.8	1.0	1.0	—

Table 1. Predictions for the $\mathcal{O}(p^4)$ low energy constants in various holographic models. The 5D integrals Y and Z are defined in eq. (2.25) and will be related to appropriate sum rules and the odd-sector $\mathcal{O}(p^6)$ LECs. The experimental determinations in χPT at $\mathcal{O}(p^4)$ are provided in the last column for comparison [2–4].

Lagrangian with the corresponding LECs given by the 5D integrals:

$$\begin{aligned} f_\pi^2 &= 4\left(\int_{-z_0}^{z_0} \frac{\mathrm{d}z}{f^2(z)}\right)^{-1}, \\ L_1 &= \frac{1}{2}L_2 = -\frac{1}{6}L_3 = \frac{1}{32}\int_{-z_0}^{z_0} \frac{(1-\psi_0^2)^2}{g^2(z)}\,\mathrm{d}z\,, \\ L_9 &= -L_{10} = \frac{1}{4}\int_{-z_0}^{z_0} \frac{1-\psi_0^2}{g^2(z)}\,\mathrm{d}z\,, \\ H_1 &= -\frac{1}{8}\int_{-z_0}^{z_0} \frac{1+\psi_0^2}{g^2(z)}\,\mathrm{d}z\,. \end{aligned} \tag{2.24}$$

The functions $f^2(z)$ and $g^2(z)$ have to satisfy some properties in order for these constants to be finite, with the exception of H_1. The numerical results for the $\mathrm{O}(p^4)$ low energy constants in four different models are collected in table 1. In the last two lines of table 1 we also provide the 5D integrals

$$\begin{aligned} Y &\equiv \int_{-z_0}^{+z_0} \frac{(1-\psi_0^4)^2}{48g^2(z)}\,\mathrm{d}z \\ Z &\equiv \int_{-z_0}^{+z_0} \frac{\psi_0^2(1-\psi_0^2)^2}{4g^2(z)}\,\mathrm{d}z \end{aligned} \tag{2.25}$$

which will appear in the next sections.

Conversely, the substitution of the $\mathcal{A}_\mu$ decomposition (2.12) in the CS action produces some operators without resonances, with only Goldstone bosons, which give rise to the Wess-Zumino-Witten (WZW) action [23, 25]:

$$S_{\mathrm{WZW}} = -\frac{iN_C}{48\pi^2}\int_{M^4} \mathcal{Z} - \frac{iN_C}{240\pi^2}\int_{M^4\times\mathbb{R}} \mathrm{tr}(g\mathrm{d}g^{-1})^5 \tag{2.26}$$

JHEP11(2012)012

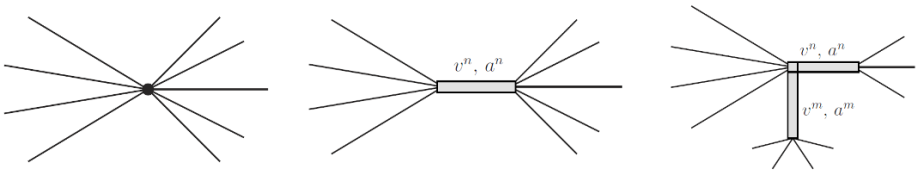

Figure 1. Examples for the different possible diagram contributing to the Goldstone interactions at low energies: a) $\mathcal{O}(p^2)$ and $\mathcal{O}(p^4)$ local interaction, b) one-resonance exchange (contribution starting at $\mathcal{O}(p^6)$), c) two or more resonance exchanges (contribution starting at $\mathcal{O}(p^8)$). The single lines represent Goldstones and the double ones resonances.

with the source-dependent terms

$$\mathcal{Z} = \langle (\ell d\ell + d\ell\ell - i\ell^3)(iU^{-1}rU - U^{-1}dU) - d\ell dU^{-1}rU - i\ell(dU^{-1}U)^3 - \frac{1}{2}(\ell dU^{-1}U)^2 - U\ell U^{-1}rdUdU^{-1} - i\ell dU^{-1}U\ell U^{-1}rU + \frac{1}{4}(\ell U^{-1}rU)^2\rangle - \text{p.c.}, \tag{2.27}$$

where "p.c." stands for the interchanges $U \leftrightarrow U^{-1}$ and $\ell \leftrightarrow r$.

3 Chiral couplings at $\mathcal{O}(p^6)$

3.1 Resonance lagrangian

We now proceed to compute the $\mathcal{O}(p^6)$ couplings at low energies. After substituting $\mathcal{A}_\mu$ in terms of the meson decomposition (2.12), the 5D action (2.1) given by the YM and CS terms contains operators with only Goldstones of at most $\mathcal{O}(p^4)$. In general we denote an operator as $\mathcal{O}(p^k)$ when it contains a number k of derivatives or external vector and axial-vector sources ($v_\mu, a_\mu \sim \partial_\mu$). The $\mathcal{O}(p^6)$ LECs are generated by the intermediate heavy resonance exchanges. More precisely, we need just the one-resonance exchanges as diagrams with a higher number of intermediate resonances will contribute to the low-energy χPT action at $\mathcal{O}(p^8)$ or beyond (see figure 1). Hence, the only operators in the Lagrangian that interest us are those containing one resonance field:

$$S_{\text{YM}}\Big|_{\text{Kin.}} = \sum_n \int \mathrm{d}^4x \langle -\frac{1}{2}(\nabla_\mu v^n_\nu - \nabla_\nu v^n_\mu)^2 + m^2_{v^n} v^{n2}_\mu - \frac{1}{2}(\nabla_\mu a^n_\nu - \nabla_\nu a^n_\mu)^2 + m^2_{a^n} a^{n2}_\mu \rangle, \tag{3.1}$$

$$\begin{aligned} S_{\text{YM}}\Big|_{1-\text{res.}} = \sum_n \int \mathrm{d}^4x \Big\{ & -\langle \frac{f_+^{\mu\nu}}{2}\Big[(\nabla_\mu v^n_\nu - \nabla_\nu v^n_\mu) a_{Vv^n} - \frac{i}{2}([u_\mu, a^n_\nu] - [u_\nu, a^n_\mu]) a_{Aa^n}\Big]\rangle \\ & -\langle \frac{i}{4}[u^\mu, u^\nu]\Big[(\nabla_\mu v^n_\nu - \nabla_\nu v^n_\mu) b_{v^n\pi\pi} - \frac{i}{2}([u_\mu, a^n_\nu] - [u_\nu, a^n_\mu]) b_{a^n\pi^3}\Big]\rangle \\ & +\langle \frac{f_-^{\mu\nu}}{2}\Big[(\nabla_\mu a^n_\nu - \nabla_\nu a^n_\mu) a_{Aa^n} - \frac{i}{2}([u_\mu, v^n_\nu] - [u_\nu, v^n_\mu])(a_{Vv^n} - b_{v^n\pi\pi})\Big]\rangle \Big\}, \end{aligned} \tag{3.2}$$

$$\begin{aligned} S_{\text{CS}}\Big|_{1-\text{res.}} = \sum_n \int \mathrm{d}^4x \Big\{ & -\frac{N_C}{32\pi^2} c_{v^n} \epsilon^{\mu\nu\alpha\beta} \langle\, u_\mu \{v^n_\nu, f_{+\alpha\beta}\}\,\rangle + \frac{N_C}{64\pi^2} c_{a^n} \epsilon^{\mu\nu\alpha\beta} \langle\, u_\mu \{a^n_\nu, f_{-\alpha\beta}\}\,\rangle \\ & + \frac{iN_C}{16\pi^2}(c_{v^n} - d_{v^n}) \epsilon^{\mu\nu\alpha\beta} \langle\, v^n_\mu u_\nu u_\alpha u_\beta\,\rangle \Big\}, \end{aligned} \tag{3.3}$$

JHEP11(2012)012

with $v_\mu^n = t^a v_\mu^{n,\,a}$, $a_\mu^n = t^a a_\mu^{n,\,a}$, and the summation over any possible n implicitly assumed. The covariant derivative is defined with the connection Γ_μ as $\nabla_\mu \,.\, = \partial_\mu + [\Gamma_\mu, .]$. The couplings are defined as

$$
\begin{aligned}
a_{Vv^n} &= \int_{-z_0}^{z_0} \frac{\psi_{2n-1}}{g^2(z)} \mathrm{d}z\,, & b_{v^n\pi\pi} &= \int_{-z_0}^{z_0} \frac{\psi_{2n-1}(1-\psi_0^2)}{g^2(z)} \mathrm{d}z \\
a_{Aa^n} &= \int_{-z_0}^{z_0} \frac{\psi_0\psi_{2n}}{g^2(z)} \mathrm{d}z\,, & b_{a^n\pi^3} &= \int_{-z_0}^{z_0} \frac{\psi_0\psi_{2n}(1-\psi_0^2)}{g^2(z)} \mathrm{d}z\,, \\
c_{v^n} &= -\frac{1}{2}\int_{-z_0}^{z_0} \psi_0\psi'_{2n-1} \mathrm{d}z\,, & d_{v^n} &= \frac{1}{2}\int_{-z_0}^{z_0} \psi_0^2\psi'_0\psi_{2n-1} \mathrm{d}z \\
c_{a^n} &= -\frac{1}{2}\int_{-z_0}^{z_0} \psi_0^2\psi'_{2n} \mathrm{d}z\,.
\end{aligned}
\tag{3.4}
$$

Notice that the a_{Vv^n} are related to the decay constants g_{v^n}, defined previously from the bulk-to-boundary propagator in eq. (2.16), in the form $g_{v^n} = m_{v^n}^2 a_{Vv^n}$. The same happens for a_{Aa^n}. Likewise, by means of the ψ_n EoM's and their b.c.'s one can extract the relations

$$
c_{v^n} = \frac{m_{v^n}^2}{2f_\pi^2} b_{v^n\pi\pi}\,, \qquad c_{a^n} = \frac{m_{a^n}^2}{3f_\pi^2} b_{a^n\pi^3}\,, \tag{3.5}
$$

$$
d_{v^n} = \frac{m_{v^n}^2}{12f_\pi^2} \int_{-z_0}^{+z_0} \frac{\psi_{2n-1}(1-\psi_0^4)}{g^2(z)} \mathrm{d}z. \tag{3.6}
$$

At the level of the generating functional, in order to compute the diagrams with intermediate resonances one must perform the functional integration over the resonance configurations. At the tree level this means that one has to find the classical solution $v_\mu^n[\pi, \ell_\mu, r_\mu]$ and $a_\mu^n[\pi, \ell_\mu, r_\mu]$ for the resonance fields in terms of the external sources and the Goldstone fields, and then substitute it in the resonance action. In the LEC analysis in this article only the terms (3.2) and (3.3) are relevant. Moreover, since we are interested in the Goldstone interaction at long distances, we need the resonance field solutions in the low-energy limit. Thus, the resonance action yields for vector and axial-vector mesons the EoM's:

$$
\begin{aligned}
v_\mu^n = -\frac{1}{2m_{v^n}^2} \Bigg(& a_{Vv^n} \nabla^\rho f_{+\rho\mu} + \frac{i}{2} b_{v^n\pi\pi} \nabla^\rho [u_\rho, u_\mu] - \frac{i}{2}(a_{Vv^n} - b_{v^n\pi\pi})[f_{-\rho\mu}, u^\rho] \\
& + \frac{N_C}{32\pi^2} c_{v^n} \epsilon_{\mu\nu\alpha\beta} \{u^\nu, f_+^{\alpha\beta}\} + \frac{iN_C}{16\pi^2}(c_{v^n} - d_{v^n}) \epsilon_{\mu\nu\alpha\beta} u^\nu u^\alpha u^\beta \Bigg)\,, \\
a_\mu^n = \frac{1}{2m_{a^n}^2} \Bigg(& a_{Aa^n} \nabla^\rho f_{-\rho\mu} + \frac{1}{4} b_{a^n\pi^3} [[u_\rho, u_\mu], u^\rho] - \frac{i}{2} a_{Aa^n} [f_{+\rho\mu}, u^\rho] \\
& + \frac{N_C}{64\pi^2} c_{a^n} \epsilon_{\mu\nu\alpha\beta} \{u^\nu, f_-^{\alpha\beta}\} \Bigg)\,,
\end{aligned}
\tag{3.7}
$$

where terms $\mathcal{O}(p^5/m_{R^n}^4)$ (with the derivatives and external vector and axial-vector sources counting as $\mathcal{O}(p)$) and two or more resonance fields are neglected on the right-hand side of the equations.

By substituting the classical field solutions (3.7) back into the resonance action from eqs. (3.1)–(3.3), one integrates out the one-resonance intermediate exchanges at the generating functional level and retrieves the corresponding $\mathcal{O}(p^6)$ Goldstone operators from

JHEP11(2012)012

the χPT Lagrangian. However, the obtained $\mathcal{O}(p^6)$ Goldstone terms do not show up directly in the chiral basis of operators commonly used in χPT [5, 6, 46]. In order to express our outcome in this form some care needs to be paid as the scalar/pseudoscalar source is absent in our holographic model. First we expand our operators using the whole operator set in refs. [5, 6, 46] and then we eliminate the terms of those operators involving the scalar/pseudoscalar source at the final step. In the even-parity sector we will see that in the absence of scalar/pseudoscalar sources it is possible to further reduce the size of $\mathcal{O}(p^6)$ operator basis. Conversely, from the study in [47] we find that in the odd-parity sector the $\mathcal{O}(p^6)$ basis chosen in refs. [46, 47] in the case when there are no scalar/pseudoscalar sources, is already minimal.

3.2 Even and odd sector sum rules

Now we discuss a series of sum rules which constrain the resonance couplings, some of which will be needed in the calculation of the LECs. They can be obtained through the 5D equation of motion (2.8) and the completeness condition (2.10). Indeed, by means of the expressions (3.4) for the resonance couplings, it is possible to introduce a double 5D integral in the infinite summation of resonance couplings. Then, thanks to the completeness condition (2.10), it is possible to eliminate the infinite resonance summation and one of the 5D integrals. We are left with a 5D integral of appropriate products of wave-function ψ_0, which can be in general related to the integrals that provide the $\mathcal{O}(p^2)$ and $\mathcal{O}(p^4)$ chiral couplings [24, 25]. Only in a few cases we were left with two new 5D integrals, Y and Z defined in (2.25). For the resonance couplings in the YM part we have:

$$\sum_{n=1}^{\infty} a_{V v^n}^2 m_{v^n}^2 - \sum_{n=1}^{\infty} a_{A a^n}^2 m_{a^n}^2 = f_\pi^2, \qquad \sum_{n=1}^{\infty} a_{V v^n}^2 - \sum_{n=1}^{\infty} a_{A a^n}^2 = -4L_{10}\,, \tag{3.8}$$

$$\sum_{n=1}^{\infty} a_{V v^n} b_{v^n \pi\pi} m_{v^n}^2 = 2f_\pi^2, \qquad \sum_{n=1}^{\infty} a_{V v^n} b_{v^n \pi\pi} = 4L_9\,, \tag{3.9}$$

$$\sum_{n=1}^{\infty} b_{v^n \pi\pi}^2 m_{v^n}^2 = \frac{4f_\pi^2}{3}, \qquad \sum_{n=1}^{\infty} b_{v^n \pi\pi}^2 = 32L_1\,, \tag{3.10}$$

$$\sum_{n=1}^{\infty} a_{A a^n} b_{a^n \pi^3} m_{a^n}^2 = 2f_\pi^2, \qquad \sum_{n=1}^{\infty} a_{A a^n} b_{a^n \pi^3} = 4L_9 - 32L_1\,, \tag{3.11}$$

$$\sum_{n=1}^{\infty} b_{a^n \pi^3}^2 m_{a^n}^2 = \frac{4f_\pi^2}{5}\,, \qquad \sum_{n=1}^{\infty} b_{a^n \pi^3}^2 = 4Z\,, \tag{3.12}$$

with Z defined in eq. (2.25). The sum rules (3.8) are related to the VV-AA correlator [19]. The relations (3.9), (3.10), (3.11) and (3.12) stem from the $\pi\pi$ vector form factor (VFF) [24], the $\pi\pi$-scattering [24], the $\pi\pi\pi$ axial-vector form factor (AFF) and the $\pi\pi\pi \to \pi\pi\pi$ scattering respectively. The $VV - AA$ correlator, VFF and $\pi\pi$-scattering sum rules have been already studied within the holographic framework in previous works [24, 25, 48]. The others involving the axial resonances are new. Especially we want to emphasize the two sum rules in eq. (3.11). They are related to the AFF into $\pi\pi\pi$, which will be studied in section 4. They can serve to improve the current phenomenological analyses on the $\pi\pi\pi$-AFF, which

JHEP11(2012)012

employ similar high-energy sum rule constraints [39, 40]. The fifth couple of sum rules (3.12) would allow us to provide a more physical meaning to the constant Z. Indeed, in the case when the summation is well defined one can use eq. (3.12) as an alternative definition of Z, in parallel with L_1 in eq. (3.10). Notice that all the sum rules involving $b_{v^n\pi\pi}$ and $b_{a^n\pi^3}$ can be reexpressed in terms of c_{v^n} and c_{a^n} through (3.5), and then are relevant for some anomalous processes.

For the other sum rules involving the anomalous couplings, only those containing $c_{v^n} - d_{v^n}$ are independent due to the resonance coupling relations (3.5). They are found to be

$$\sum_{n=1}^{\infty} \frac{c_{v^n}(c_{v^n}-d_{v^n})}{m_{v^n}^2} = \frac{4}{15f_\pi^2}\,, \qquad \sum_{n=1}^{\infty} \frac{c_{v^n}(c_{v^n}-d_{v^n})}{m_{v^n}^4} = \frac{1}{6f_\pi^4}\,(40L_1 - Z)\,, \tag{3.13}$$

$$\sum_{n=1}^{\infty} \frac{(c_{v^n}-d_{v^n})^2}{m_{v^n}^2} = \frac{68}{315f_\pi^2}\,, \qquad \sum_{n=1}^{\infty} \frac{(c_{v^n}-d_{v^n})^2}{m_{v^n}^4} = \frac{1}{3f_\pi^4}\,(16L_1 - Z + Y)\,, \tag{3.14}$$

$$\sum_{n=1}^{\infty} a_{Vv^n}(c_{v^n}-d_{v^n}) = \frac{2}{3}\,, \qquad \sum_{n=1}^{\infty} \frac{a_{Vv^n}(c_{v^n}-d_{v^n})}{m_{v^n}^2} = \frac{4}{3f_\pi^2}(2L_1 + L_9)\,. \tag{3.15}$$

The first two sum rules are related to a set of diagrams in the vector form factor into four pions, or $\pi\pi \to \pi\pi\pi$ scattering replacing c_{v^n} with $b_{v^n\pi\pi}$. The second two appear, for instance, in the scattering $\pi\pi\pi \to \pi\pi\pi$, while the last two can be related to the vector form factor into three pions.

These sum rules perform a summation over the infinite tower of resonances, and in principle one may wonder how well the first terms of the series reproduce the full result. The reason is that, in spite of the fact of having an infinite number of hadrons in the large-N_C limit of QCD [49–51], in the majority of the hadronic analyses only the lightest states are taken into account, introducing a "truncation" error. Many authors have investigated the importance of the lightest resonances in the summation [13, 52–55]. Since the development of the Weinberg sum rules [56, 57], the relations (3.8)–(3.15) have been truncated at their lowest orders and have been used to make predictions on hadronic phenomenology [16]. Some authors have nonetheless argued about the relevance of the tail of the series and the numerical (and also theoretical) impact of the higher terms of the series on the QCD amplitudes at low and intermediate energies [13, 55]. For this reason, we consider that the study of the saturation of the presented sum rules may be useful for most of the phenomenological studies, which only include the lightest hadrons. Indeed, the first constraints (3.8)–(3.10) have been previously obtained in the case of resonance Lagrangians from the analysis of the high-energy behavior of the $VV-AA$ correlator ($F_V^2 - F_A^2 = f_\pi^2$) [16, 56, 57], the $\pi\pi$ VFF ($F_V G_V = f_\pi^2$) [16] and the $\pi\pi$-scattering ($3\,G_V^2 = f_\pi^2$) [58, 59], where the corresponding couplings are related to those used in this paper through $F_V = a_{V\rho} m_\rho$, $F_A = a_{Aa_1} m_{a_1}$ and $G_V = b_{\rho\pi\pi} m_\rho/2$.

In table 2 we check how well the sum rules (3.8)–(3.15) are saturated by the lightest resonance multiplets of vectors and axial-vectors. The second sum rule in every line in eqs. (3.8)–(3.15) is always much better saturated by the lightest meson than the first one, as it contains an extra $1/m_{R^n}^2$ suppression. One can see that, in general, the first term of the series already provides a reasonable approximation. The only exception is the $VV-AA$

JHEP11(2012)012

	Flat	Cosh	Hard-wall	Sakai-Sugimoto
$1-\frac{a_{V\rho}^2 m_\rho^2 - a_{Aa_1}^2 m_{a_1}^2}{\Sigma_n (a_{Vv^n}^2 m_{v^n}^2 - a_{Aa^n}^2 m_{a^n}^2)}$	99 %	300 %	350 %	840 %
$1-\frac{a_{V\rho}^2 - a_{Aa_1}^2}{\sum_n (a_{Vv^n}^2 - a_{Aa^n}^2)}$	8 %	34 %	41 %	110 %
$1-\frac{a_{V\rho} b_{\rho\pi\pi} m_\rho^2}{\Sigma_n a_{Vv^n} b_{v^n\pi\pi} m_{v^n}^2}$	18 %	0	-11 %	-30 %
$1-\frac{a_{V\rho} b_{\rho\pi\pi}}{\Sigma_n a_{Vv^n} b_{v^n\pi\pi}}$	0.8 %	0	-2 %	-6 %
$1-\frac{3 b_{\rho\pi\pi}^2 m_\rho^2}{\Sigma_n 3 b_{v^n\pi\pi}^2 m_{v^n}^2}$	0.7 %	0	0.7 %	2 %
$1-\frac{b_{\rho\pi\pi}^2}{\Sigma_n b_{v^n\pi\pi}^2}$	-0.6 %	0	0.2 %	1 %
$1-\frac{a_{Aa_1} b_{a_1\pi^3} m_{a_1}^2}{\Sigma_n a_{Aa^n} b_{a^n\pi^3} m_{a^n}^2}$	39 %	0	-11 %	-54 %
$1-\frac{a_{Aa_1} b_{a_1\pi^3}}{\Sigma_n a_{Aa^n} b_{a^n\pi^3}}$	8 %	0	-3.4 %	-15 %
$1-\frac{5 b_{a_1\pi^3}^2 m_{a_1}^2}{\Sigma_n 5 b_{a^n\pi^3}^2 m_{a^n}^2}$	8 %	0	0.8 %	6 %
$1-\frac{b_{a_1\pi^3}^2}{\Sigma_n b_{a^n\pi^3}^2}$	2 %	0	0.2 %	2 %
$1-\frac{c_\rho(c_\rho - d_\rho)/m_\rho^2}{\Sigma_n c_{v^n}(c_{v^n} - d_{v^n})/m_{v^n}^2}$	2 %	0	1.5 %	4 %
$1-\frac{c_\rho(c_\rho - d_\rho)/m_\rho^4}{\Sigma_n c_{v^n}(c_{v^n} - d_{v^n})/m_{v^n}^4}$	0.3 %	0	0.3 %	1.4 %
$1-\frac{(c_\rho - d_\rho)^2/m_\rho^2}{\sigma_n (c_{v^n} - d_{v^n})^2/m_{v^n}^2}$	3 %	0.1 %	3 %	6 %
$1-\frac{(c_\rho - d_\rho)^2/m_\rho^4}{(c_{v^n} - d_{v^n})^2/m_{v^n}^4}$	0.6 %	-0.6 %	0.6 %	2 %
$1-\frac{a_{V\rho}(c_\rho - d_\rho)}{\Sigma_n a_{Vv^n}(c_{v^n} - d_{v^n})}$	- 30 %	- 20 %	-30 %	-50 %
$1-\frac{a_{V\rho}(c_\rho - d_\rho)/m_\rho^2}{\Sigma_n a_{Vv^n}(c_{v^n} - d_{v^n})/m_{v^n}^2}$	- 5 %	- 3 %	-5 %	-10 %

Table 2. Analysis of the saturation of the sum rules (3.8)–(3.15) by the first resonance multiplets $\rho(770)$ and $a_1(1260)$. The denominators $\Sigma_n(\ldots)$ represent the resummed expression for the summations from $n=1$ up to ∞ provided in eqs. (3.8)–(3.15).

JHEP11(2012)012

Weinberg sum rules in eq. (3.8), which is found to be badly convergent. Indeed, in the asymptotically anti-de Sitter (AdS) models we are studying ("Cosh" [19] and hard-wall [24]) the resonance masses and couplings scale, respectively, as $m^2_{v^n}, m^2_{a^n} \sim n^2$ and $a^2_{Vv^n}, a^2_{Aa^n} \sim n^{-1}$: the first WSR — first constraint in eq. (3.8) — is not convergent and, even though the alternate series in the second sum rule in eq. (3.8) is convergent, it is not absolutely convergent.[1] This kind of pathologies are softened in the case of soft-wall models with a quadratic dilaton [60–62], as they recover the linear Regge trajectories $m^2_{v^n}, m^2_{a^n} \sim n$ and $a^2_{Vv^n}, a^2_{Aa^n} \sim n^{-1}$.

3.3 Odd-intrinsic parity LECs

Now we are ready to show the results for the $\mathcal{O}(p^6)$ LECs in the odd sector. After expressing the outcome in the $\mathcal{O}(p^6)$ basis of odd-parity operators provided in ref. [46], we obtain the predictions:

$$
\begin{aligned}
C_{12}^W &= -\frac{N_C}{128\pi^2} S_{\pi^5}, & C_{13}^W &= \frac{N_C}{64\pi^2}(\tilde{S}_{V\pi^3} - S_{V\pi^3} - S_{\pi VV}),\\
C_{14}^W &= \frac{N_C}{128\pi^2}(\tilde{S}_{V\pi^3} - S_{\pi VV}), & C_{15}^W &= \frac{N_C}{128\pi^2}(2\tilde{S}_{V\pi^3} + S_{V\pi^3} - S_{\pi VV}),\\
C_{16}^W &= \frac{N_C}{128\pi^2}(3S_{\pi^5} - 2S_{V\pi^3} - S_{A\pi^4}), & C_{17}^W &= \frac{N_C}{512\pi^2}(6\tilde{S}_{V\pi^3} - 4S_{\pi VV} - S_{A\pi^4}),\\
C_{19}^W &= -\frac{N_C}{128\pi^2}(2S_{V\pi^3} + S_{\pi AA}), & C_{20}^W &= \frac{N_C}{256\pi^2}(6\tilde{S}_{V\pi^3} - 4S_{\pi VV} - S_{\pi AA}),\\
C_{21}^W &= \frac{N_C}{256\pi^2}(2S_{V\pi^3} - S_{\pi AA}), & C_{22}^W &= \frac{N_C}{64\pi^2} S_{\pi VV},\\
C_{23}^W &= \frac{N_C}{128\pi^2} S_{\pi AA}, & &
\end{aligned}
\tag{3.16}
$$

with the summations over resonances,

$$
\begin{aligned}
S_{\pi VV} &= \sum_{n=1}^{\infty} \frac{a_{Vv^n} c_{v^n}}{m^2_{v^n}}, & S_{\pi AA} &= \sum_{n=1}^{\infty} \frac{a_{Aa^n} c_{a^n}}{m^2_{a^n}},\\
S_{V\pi^3} &= \sum_{n=1}^{\infty} \frac{a_{Vv^n}}{m^2_{v^n}}(c_{v^n} - d_{v^n}), & \tilde{S}_{V\pi^3} &= \sum_{n=1}^{\infty} \frac{c_{v^n} b_{v^n \pi\pi}}{m^2_{v^n}},\\
S_{\pi^5} &= \sum_{n=1}^{\infty} \frac{b_{v^n \pi\pi}}{m^2_{v^n}}(c_{v^n} - d_{v^n}), & S_{A\pi^4} &= \sum_{n=1}^{\infty} \frac{c_{a^n} b_{a^n \pi^3}}{m^2_{a^n}},
\end{aligned}
\tag{3.17}
$$

which one may find in the sum rules (3.8)–(3.15) with the help of the resonance coupling relations (3.5). Hence, all the odd intrinsic-parity LECs can be expressed through L_1, L_9

[1] The convergence behavior is slightly better in the case of flat metric [19] and worse in the Sakai-Sugimoto model [23, 25]. In the flat model [19] one has the high-energy behavior $\Pi_{VV}, \Pi_{AA} \sim 1/Q$ and $a^2_{Vv^n}, a^2_{Aa^n} \sim n^{-2}$ for large n. On the other hand, in the Sakai-Sugimoto case [23, 25] one has $\Pi_{VV}, \Pi_{AA} \sim Q$ and $a^2_{Vv^n}, a^2_{Aa^n} \sim n^0$. In all the holographic theories considered here [19, 23–25] the resonance masses behave like $m^2_{v^n}, m^2_{a^n} \sim n^2$ for high n. The dependence of the masses and couplings on the excitation number n in the different models can be found in appendix. A.

JHEP11(2012)012

and the constant Z (defined in (2.25)):

$$C_{12}^W = -\frac{N_C}{384\pi^2 f_\pi^2}(40L_1 - Z) \tag{3.18}$$

$$C_{13}^W = \frac{5N_C}{96\pi^2 f_\pi^2}(4L_1 - L_9) \tag{3.19}$$

$$C_{14}^W = \frac{N_C}{64\pi^2 f_\pi^2}(8L_1 - L_9) \tag{3.20}$$

$$C_{15}^W = \frac{N_C}{192\pi^2 f_\pi^2}(52L_1 - L_9) \tag{3.21}$$

$$C_{16}^W = \frac{N_C}{384\pi^2 f_\pi^2}(104L_1 - 8L_9 - 7Z) \tag{3.22}$$

$$C_{17}^W = \frac{N_C}{384\pi^2 f_\pi^2}(72L_1 - 6L_9 - Z) \tag{3.23}$$

$$C_{19}^W = \frac{N_C}{96\pi^2 f_\pi^2}(4L_1 - 3L_9) \tag{3.24}$$

$$C_{20}^W = \frac{N_C}{192\pi^2 f_\pi^2}(80L_1 - 7L_9) \tag{3.25}$$

$$C_{21}^W = \frac{N_C}{192\pi^2 f_\pi^2}(12L_1 + L_9) \tag{3.26}$$

$$C_{22}^W = \frac{N_C}{32\pi^2 f_\pi^2}L_9 \tag{3.27}$$

$$C_{23}^W = \frac{N_C}{96\pi^2 f_\pi^2}(L_9 - 8L_1). \tag{3.28}$$

The $1/N_C$ subleading coupling C_{18}^W and those related to operators with scalar/pseudoscalar sources do not appear. This set of equations provides a relation between the even and odd-parity sectors of QCD. Actually, taking into account that $L_9 = -L_{10}$ [24, 25], we recover the result $C_{22}^W = -\frac{N_C}{32\pi^2 f_\pi^2}L_{10}$ previously derived through the low-energy expansion of the Son-Yamamoto relation [37].

We provide in table 3 the numerical results for the four holographic models mentioned before. Among them, the "Cosh" model accommodates better the low-energy inputs and the required gauge coupling value g_5 needed to recover the right coefficient for the pQCD log of the two-points correlators [19]. Thus we take this as our preferred set of estimates. Nonetheless, it is worthy to remark that the LEC predictions from the various models considered here are relatively stable, with variations between one and another of the order of $\sim 1 \cdot 10^{-3}\,\mathrm{GeV}^{-2}$, similar to the renormalization μ scale dependence of the $\mathcal{O}(p^6)$ LECs in χPT [46]. In cases like C_{12}^W, C_{15}^W or C_{21}^W the shift is pretty small, while for others like C_{13}^W, C_{19}^W or C_{20}^W one sees larger oscillations depending on the models at hand.

Along the years, many analyses have been devoted to the study of QCD amplitudes under the minimal hadronical approximation [52–54], where one considers just the lightest multiplets of resonances entering in the problem at hand. A recent study of the low-energy contributions from a general odd-intrinsic resonance Lagrangian with only the lightest me-

JHEP11(2012)012

	Flat	"Cosh"	Hard-wall	Sakai-Sugimoto
C_{12}^W	-2.1	-2.1	-2.1	-2.1
C_{13}^W	-6.5	-8.8	-9.9	-11.9
C_{14}^W	-0.6	-1.3	-1.7	-2.3
C_{15}^W	4.5	4.4	4.2	4.0
C_{16}^W	0.9	-0.2	-0.8	-1.6
C_{17}^W	0.6	-0.1	-0.5	-1.1
C_{19}^W	-5.6	-7.0	-7.7	-8.8
C_{20}^W	1.1	-0.4	-1.3	-2.3
C_{21}^W	2.4	2.6	2.7	2.9
C_{22}^W	6.5	7.9	8.6	9.7
C_{23}^W	0.4	0.9	1.1	1.5

Table 3. Numerical results for the $\mathcal{O}(p^6)$ low energy constants in the odd sector from different holographic models. The $\mathcal{O}(p^6)$ LECs are in units of $10^{-3}\,\text{GeV}^{-2}$.

	"Cosh"	DSE [18]	χPT	CQM [8]	Res. Lagr.	VMD
C_{12}^W	-2.1	$-5.13^{+0.15}_{-0.25}$			-4.3 ± 0.3 [63]	
C_{13}^W	-8.8	$-6.37^{+0.18}_{-0.31}$	-70 ± 60 [8]	14 ± 15		-20.0 [8]
			-10 ± 70 [8]	-7 ± 20		
C_{14}^W	-1.3	$-2.00^{+0.06}_{-0.10}$	30 ± 11 [8]	10 ± 8		-6.0 [8]
			1 ± 15 [8]	-1 ± 10		
C_{15}^W	4.4	$4.17^{+0.12}_{-0.20}$	-25 ± 24 [8]	20 ± 7		2.0 [8]
			-3 ± 29 [8]	9 ± 10		
C_{16}^W	-0.2	$3.58^{+0.10}_{-0.17}$				
C_{17}^W	-0.1	$1.98^{+0.06}_{-0.10}$				
C_{19}^W	-7.0	$0.29^{+0.01}_{-0.01}$				
C_{20}^W	-0.4	$1.83^{+0.05}_{-0.09}$				
C_{21}^W	2.6	$2.48^{+0.07}_{-0.12}$				
C_{22}^W	7.9	$5.01^{+0.14}_{-0.24}$	6.5 ± 0.8 [8]	3.9 ± 0.4	8.0 [64]	8.0 [65–67]
			5.1 ± 0.7 [8]		6.5 [68]	
			5.4 ± 0.8 [69]		8.1 ± 0.8 [70]	
			$7.0^{+1.0}_{-1.5}$ [71]			
C_{23}^W	0.9	$2.74^{+0.08}_{-0.13}$				

Table 4. Numerical results for the odd-intrinsic parity $\mathcal{O}(p^6)$ low energy constants within the "Cosh" model compared to alternative determinations in other frameworks: Dyson-Schwinger Equation (DSE) [18], χPT [8, 69], Constituent Chiral Quark Model (CQM) [8], Hidden Local Symmetry [63], Resonance Chiral Theory [64, 68, 71], rational approximations [70] and Vector Meson Dominance (VMD) [8, 65–67]. The $\mathcal{O}(p^6)$ LECs are given in units of 10^{-3} GeV^{-2}.

JHEP11(2012)012

son multiplets has led to the relation [64]

$$\frac{F_V^2}{2G_V}C_{12}^W \,-\, F_V(C_{14}^W - C_{15}^W) \,=\, G_V C_{22}^W \,. \tag{3.29}$$

One can verify that this is a direct consequence of our results (3.16) when keeping only the lightest resonance multiplets in the sums (3.17) involved. Since all the sums are well saturated by the lowest multiplets, as shown in the previous subsection, this relation should be reasonably satisfied with the exact values of the couplings. We have checked that this relation is pretty well fulfilled for various holographic models, with deviations that vary from 1% in the flat background to 11% in the Sakai-Sugimoto model.

One can also compare our predictions with previous phenomenological determinations in various frameworks. The full set of $\mathcal{O}(p^6)$ LECs was computed in ref. [18] by means of the DSE. Other approaches are based on the analysis of experimental decays and anomalous processes directly through χPT [8, 69], although in general the determinations are not very precise except for C_{22}^W. Alternatively, several authors have estimated LECs by considering just the lightest multiplet of resonances in the effective Lagrangian [63, 64, 68], rational approximations [70] and the assumption of vector meson dominance (VMD) [8, 65–67]. All these results are compared in table 4. There are some couplings ($C_{16}^W \,\ldots\, C_{21}^W$, C_{23}^W) that, except for the DSE computation [18], are completely unknown, so that the present work may help further explorations of anomalous QCD amplitudes. One has to take into account that variations of the renormalization scale μ induce shifts in the physical $\mathcal{O}(p^6)$ chiral couplings in the form [46]

$$\frac{dC_k^W}{d\ln\mu^2} \,=\, -\,\frac{\eta_k}{32\pi^2}\,, \tag{3.30}$$

with $\left|\frac{\eta_k}{32\pi^2}\right| \sim 1\cdot 10^{-3}\,\text{GeV}^{-2}$ [46]. Hence, no comparison to a large-N_C estimate can claim an absolute precision beyond that. In most cases, we find a reasonable agreement with the few previous determinations. Some LECs like C_{15}^W and C_{21}^W agree extremely well with the DSE determinations. Conversely, the predictions for other couplings like C_{19}^W seem to be far more spread. In any case, with the exception of C_{22}^W which is relatively well know from the $\pi^0 \to \gamma\gamma^*$ decay, the remaining estimates carry large uncertainties, if known at all, so our results are expected to be of help for the development of the study of the anomalous sector of QCD.

3.4 Even-intrinsic parity LECs

For the even-parity sector we proceed in a similar way. Our results for the constants in the three-flavor notation are listed in table 5.

Here the chiral couplings are given in terms of the summations over resonance exchanges,

$$\begin{aligned}
S_{VV} &= \sum_{n=1}^{\infty}\frac{a_{Vv^n}^2}{m_{v^n}^2}\,, \qquad S_{V\pi\pi} = \sum_{n=1}^{\infty}\frac{a_{Vv^n}b_{v^n\pi\pi}}{m_{v^n}^2}\,, \qquad S_{\pi^4} = \sum_{n=1}^{\infty}\frac{b_{v^n\pi\pi}^2}{m_{v^n}^2}\,,\\
S_{AA} &= \sum_{n=1}^{\infty}\frac{a_{Aa^n}^2}{m_{a^n}^2}\,, \qquad S_{A\pi^3} = \sum_{n=1}^{\infty}\frac{a_{Aa^n}b_{a^n\pi^3}}{m_{a^n}^2}\,, \qquad S_{\pi^6} = \sum_{n=1}^{\infty}\frac{b_{a^n\pi^3}^2}{m_{a^n}^2}\,.
\end{aligned} \tag{3.31}$$

JHEP11(2012)012

C_1	$-\frac{1}{4}S_{A\pi^3}+\frac{1}{32}S_{\pi^4}$
C_3	$\frac{1}{16}S_{A\pi^3}$
C_4	$-\frac{3}{16}S_{A\pi^3}+\frac{1}{32}S_{\pi^4}$
C_{40}	$\frac{1}{4}S_{A\pi^3}-\frac{1}{32}S_{\pi^4}-\frac{1}{32}S_{\pi^6}$
C_{42}	$\frac{1}{8}S_{A\pi^3}-\frac{1}{32}S_{\pi^4}-\frac{1}{32}S_{\pi^6}+\frac{17N_C^2}{80640\pi^4 f_\pi^2}$
C_{44}	$-\frac{1}{2}S_{A\pi^3}+\frac{1}{16}S_{\pi^4}+\frac{1}{8}S_{\pi^6}-\frac{17N_C^2}{40320\pi^4 f_\pi^2}$
C_{46}	$-\frac{1}{8}S_{A\pi^3}-\frac{17N_C^2}{80640\pi^4 f_\pi^2}$
C_{47}	$\frac{1}{4}S_{A\pi^3}-\frac{1}{16}S_{\pi^6}+\frac{17N_C^2}{40320\pi^4 f_\pi^2}$
C_{48}	$\frac{1}{16}S_{A\pi^3}-\frac{1}{32}S_{\pi^4}+\frac{N_C^2}{1920\pi^4 f_\pi^2}$
C_{50}	$\frac{1}{4}S_{A\pi^3}+\frac{1}{8}S_{V\pi\pi}+\frac{N_C^2}{960\pi^4 f_\pi^2}$
C_{51}	$\frac{3}{8}S_{A\pi^3}-\frac{1}{16}S_{\pi^4}+\frac{1}{8}S_{V\pi\pi}$
C_{52}	$-\frac{1}{8}S_{V\pi\pi}-\frac{N_C^2}{1920\pi^4 f_\pi^2}$
C_{53}	$\frac{3}{16}S_{AA}-\frac{1}{16}S_{V\pi\pi}-\frac{3}{16}S_{VV}+\frac{N_C^2}{3072\pi^4 f_\pi^2}$
C_{55}	$-\frac{3}{16}S_{AA}+\frac{1}{16}S_{V\pi\pi}+\frac{3}{16}S_{VV}+\frac{N_C^2}{3072\pi^4 f_\pi^2}$
C_{56}	$-\frac{3}{8}S_{AA}-\frac{1}{8}S_{V\pi\pi}+\frac{3}{8}S_{VV}-\frac{N_C^2}{1536\pi^4 f_\pi^2}$
C_{57}	$-\frac{1}{8}S_{AA}+\frac{1}{4}S_{V\pi\pi}+\frac{1}{8}S_{VV}$
C_{59}	$\frac{1}{4}S_{AA}-\frac{1}{16}S_{V\pi\pi}-\frac{1}{4}S_{VV}-\frac{N_C^2}{3072\pi^4 f_\pi^2}$
C_{66}	$-\frac{1}{16}S_{A\pi^3}+\frac{3}{32}S_{\pi^4}-\frac{1}{16}S_{V\pi\pi}$
C_{69}	$\frac{1}{16}S_{A\pi^3}-\frac{3}{32}S_{\pi^4}+\frac{1}{16}S_{V\pi\pi}$
C_{70}	$-\frac{1}{8}S_{AA}+\frac{3}{8}S_{A\pi^3}-\frac{1}{32}S_{\pi^4}-\frac{1}{16}S_{V\pi\pi}+\frac{1}{8}S_{VV}+\frac{N_C^2}{46080\pi^4 f_\pi^2}$
C_{72}	$\frac{1}{8}S_{AA}-\frac{3}{16}S_{A\pi^3}+\frac{1}{16}S_{V\pi\pi}-\frac{1}{8}S_{VV}+\frac{N_C^2}{46080\pi^4 f_\pi^2}$
C_{73}	$\frac{1}{8}S_{AA}-\frac{1}{2}S_{A\pi^3}+\frac{1}{8}S_{V\pi\pi}-\frac{1}{8}S_{VV}-\frac{N_C^2}{23040\pi^4 f_\pi^2}$
C_{74}	$\frac{1}{8}S_{AA}+\frac{3}{8}S_{A\pi^3}-\frac{5}{16}S_{\pi^4}-\frac{1}{8}S_{V\pi\pi}-\frac{1}{8}S_{VV}$
C_{76}	$-\frac{1}{8}S_{AA}+\frac{1}{4}S_{A\pi^3}+\frac{1}{8}S_{\pi^4}+\frac{1}{8}S_{VV}-\frac{N_C^2}{46080\pi^4 f_\pi^2}$
C_{78}	$-\frac{1}{4}S_{AA}+\frac{1}{16}S_{V\pi\pi}+\frac{1}{4}S_{VV}$
C_{79}	$-\frac{1}{8}S_{AA}-\frac{1}{16}S_{V\pi\pi}+\frac{1}{8}S_{VV}$
C_{87}	$-\frac{1}{8}S_{AA}+\frac{1}{8}S_{VV}$
C_{88}	$-\frac{1}{8}S_{V\pi\pi}$
C_{89}	$-\frac{1}{4}S_{AA}+\frac{3}{8}S_{V\pi\pi}+\frac{1}{4}S_{VV}$
C_{92}	S_{VV}
C_{93}	$-\frac{1}{4}S_{VV}$

Table 5. Holographic predictions for the $\mathcal{O}(p^6)$ LECs in the even sector.

JHEP11(2012)012

With the help of the decomposition (2.18) of the Green function, we can write these sums in the form

$$\begin{aligned}
S_{VV} &= \int_{-z_0}^{+z_0} \mathrm{d}z \int_{-z_0}^{+z_0} \mathrm{d}z' \frac{G(0,z,z')}{g^2(z)g^2(z')} \\
S_{V\pi\pi} &= \int_{-z_0}^{+z_0} \mathrm{d}z \int_{-z_0}^{+z_0} \mathrm{d}z' \frac{G(0,z,z')(1-\psi_0(z)^2)}{g^2(z)g^2(z')}, \\
S_{\pi^4} &= \int_{-z_0}^{+z_0} \mathrm{d}z \int_{-z_0}^{+z_0} \mathrm{d}z' \frac{G(0,z,z')(1-\psi_0(z)^2)(1-\psi_0(z')^2)}{g^2(z)g^2(z')} \\
S_{AA} &= \int_{-z_0}^{+z_0} \mathrm{d}z \int_{-z_0}^{+z_0} \mathrm{d}z' \frac{G(0,z,z')\psi_0(z)\psi_0(z')}{g^2(z)g^2(z')} \\
S_{A\pi^3} &= \int_{-z_0}^{+z_0} \mathrm{d}z \int_{-z_0}^{+z_0} \mathrm{d}z' \frac{G(0,z,z')\psi_0(z')\psi_0(z)(1-\psi_0(z)^2)}{g^2(z)g^2(z')} \\
S_{\pi^6} &= \int_{-z_0}^{+z_0} \mathrm{d}z \int_{-z_0}^{+z_0} \mathrm{d}z' \frac{G(0,z,z')\psi_0(z)(1-\psi_0(z)^2)\psi_0(z')(1-\psi_0(z')^2)}{g^2(z)g^2(z')}.
\end{aligned} \tag{3.32}$$

They can be calculated through the expression (2.22) once ψ_0 is known. In deriving the low energy constants in table 5 we have also used the sum rules (3.13) and (3.14), which allow us to express all the contributions from the odd intrinsic parity resonance sector in terms of just f_π. These odd-sector terms were not considered in previous RχT estimates of the $\mathcal{O}(p^6)$ chiral couplings [72, 73].

In table 5 we find contributions for all the even-sector χPT operators at $\mathcal{O}(p^6)$ which do not contain scalar/pseudoscalar sources except for a few of them:

$$\begin{aligned}
0 \;=\; C_2 \;=\; C_{41} \;=\; C_{43} \;=\; C_{45} \;=\; C_{49} \;=\; C_{54} \;=\; C_{58} \\
= C_{60} = C_{67} = C_{68} = C_{71} = C_{75} = C_{77}\,.
\end{aligned} \tag{3.33}$$

They correspond to multi-trace operators and are suppressed by $1/N_C$. In addition, we obtain $C_{90} = 0$, which we want to discuss here in more details. If scalar-pseudoscalar sources χ are not included in χPT ($\chi = 0$), the basis of $\mathcal{O}(p^6)$ even operators can be further simplified beyond the trivial simplifications $\mathcal{O}_{5,\ldots 39} = \mathcal{O}_{61,\ldots 65} = \mathcal{O}_{80,\ldots 86} = \mathcal{O}_{91,94} = 0$. In the usual χPT computation with scalar-pseudoscalar sources we have the SU(3) operator relation [5, 6]

$$\begin{aligned}
-\langle\, f_{+\,\mu\nu}[\chi_-^\mu, u^\nu]\,\rangle = \Big[&\mathcal{O}_{50} + \mathcal{O}_{51} - \mathcal{O}_{52} - \frac{1}{2}\mathcal{O}_{53} + \frac{1}{2}\mathcal{O}_{55} - \mathcal{O}_{56} + 2\mathcal{O}_{57} - \frac{1}{2}\mathcal{O}_{59} \\
&- \frac{1}{2}\mathcal{O}_{70} + \frac{1}{2}\mathcal{O}_{72} + \mathcal{O}_{73} - \frac{1}{2}\mathcal{O}_{76} + \frac{1}{2}\mathcal{O}_{78} - \frac{1}{2}\mathcal{O}_{79} - \mathcal{O}_{88} - \mathcal{O}_{90} \Big] \\
&+ \Big[\frac{1}{2}\mathcal{O}_{63} + \mathcal{O}_{65} + \frac{1}{4}\mathcal{O}_{104} \Big],
\end{aligned} \tag{3.34}$$

with $\chi_-^\mu = \nabla^\mu \chi_- - \frac{i}{2}\{\chi_+, u^\mu\}$ [5, 6]. The operators in the second bracket on the right-hand side of (3.34) contain the tensor χ and, hence, in the absence of scalar-pseudoscalar sources

JHEP11(2012)012

the basis of $\mathcal{O}(p^6)$ operators can be simplified through the relation

$$0 = \Big[\mathcal{O}_{50} + \mathcal{O}_{51} - \mathcal{O}_{52} - \frac{1}{2}\mathcal{O}_{53} + \frac{1}{2}\mathcal{O}_{55} - \mathcal{O}_{56} + 2\mathcal{O}_{57} - \frac{1}{2}\mathcal{O}_{59} - \frac{1}{2}\mathcal{O}_{70} + \frac{1}{2}\mathcal{O}_{72} + \mathcal{O}_{73} - \frac{1}{2}\mathcal{O}_{76} + \frac{1}{2}\mathcal{O}_{78} - \frac{1}{2}\mathcal{O}_{79} - \mathcal{O}_{88} - \mathcal{O}_{90} \Big] . \tag{3.35}$$

Therefore, when one describes QCD matrix elements in the chiral limit without scalar-pseudoscalar sources — as we do in the present article — the number of independent operators is actually smaller than that one would naively assume. Thus, for instance, if one removes the operator $\mathcal{O}_{90}$ from the minimal basis, we find that the only physical combinations of $\mathcal{O}(p^6)$ couplings one may determine in the $\chi = 0$ case are

$$\begin{aligned} &C_{50} + C_{90} , \quad C_{51} + C_{90} , \quad C_{52} - C_{90} , \quad C_{53} - \frac{1}{2}C_{90} , \quad C_{55} + \frac{1}{2}C_{90} , \\ &C_{56} - C_{90} , \quad C_{57} + 2C_{90} , \quad C_{59} - \frac{1}{2}C_{90} , \quad C_{70} - \frac{1}{2}C_{90} , \quad C_{72} + \frac{1}{2}C_{90} , \\ &C_{73} + C_{90} , \quad C_{76} - \frac{1}{2}C_{90} , \quad C_{78} + \frac{1}{2}C_{90} , \quad C_{79} - \frac{1}{2}C_{90} , \quad C_{88} - C_{90} , \end{aligned} \tag{3.36}$$

and the remaining couplings not listed in (3.34). We want to remark that our analysis of the $\mathcal{O}(p^6)$ operators in the absence of scalar-pseudoscalar sources is not exhaustive, and more relations might be found, allowing a further reduction of the $\mathcal{O}(p^6)$ basis.

There are combinations of couplings where the sums over the resonances can be eliminated. In particular, in the comparison with the phenomenology there are a few relations of interest:

$$\begin{aligned} 3C_3 + C_4 &= C_1 + 4C_3 , \\ 2C_{78} - 4C_{87} + C_{88} &= 0 , \\ 8C_{53} + 8C_{55} + C_{56} + C_{57} + 2C_{59} &= \frac{N_C^2}{256\pi^4 f_\pi^2} , \\ C_{56} + C_{57} + 2C_{59} &= -\frac{N_C^2}{768\pi^4 f_\pi^2} , \\ 8C_{53} - 8C_{55} + C_{56} + C_{57} - 2C_{59} + 4C_{78} + 8C_{87} - 4C_{88} &= 0 , \\ C_{56} + C_{57} - 2C_{59} - 4C_{78} &= 0 . \end{aligned} \tag{3.37}$$

The first relation is connected to the $\pi\pi$ scattering, and the combination of LECs in the second line yields the contribution to the axial-vector form factor to $\pi\gamma$, $G_A(Q^2)$, at $\mathcal{O}(p^6)$ in the chiral limit [6]. Actually, this form factor vanishes identically in this class of models, $G_A(Q^2) = 0$ [24]. This is one example of those universal relations of amplitudes in these models, which will be studied further in the next section. The relation is not in serious conflict with experiments since the branching ratio of the relevant decay $\pi^+ \to l^+\nu\gamma$ is suppressed by more than two orders of magnitude with respect to the dominant decay channel $\pi^+ \to \mu^+\nu$. At $\mathcal{O}(p^4)$, it leads to the identity $L_9 + L_{10} = 0$ shown before. From the view of resonance exchanges, one finds that all the decay amplitudes $a^n \to \pi\gamma$ vanish [24, 25]. These decay amplitudes receive contributions from the $\langle f_+^{\mu\nu}[u_\mu, a_\nu^n]\rangle$ and $\langle f_-^{\mu\nu}\nabla_\mu a_\nu^n\rangle$

JHEP11(2012)012

terms in the resonance Lagrangian (3.3), which have the same coupling and cancel exactly with each other [24]. Actually, in the original hidden local symmetry model with the lightest resonance multiplets [74], no $a_1 \to \pi\gamma$ decay occurs. Moreover, in the holographic framework where a scalar field dual to the quark condensate is introduced, these amplitudes also vanish [27]. Experimentally the partial width if $a_1 \to \pi\gamma$ is very small compared to the total width, so it is supposed to be induced by some higher derivative terms or $1/N_C$ suppressed terms [19, 24, 25, 27].

The other relations are connected to the photon-photon collision. For the $\gamma\gamma \to \pi^0\pi^0$ process, the following quantities are introduced [75]:

$$\begin{aligned} a_2^{00} &= 256\pi^4\ f_\pi^2\ (8C_{53} + 8C_{55} + C_{56} + C_{57} + 2C_{59})\,, \\ b^{00} &= -128\pi^4\ f_\pi^2\ (C_{56} + C_{57} + 2C_{59})\,. \end{aligned} \tag{3.38}$$

For $\gamma\gamma \to \pi^+\pi^-$ a similar set of quantities are defined [76]:

$$\begin{aligned} a_2^{+-} &= 256\pi^4\ f_\pi^2\ (8C_{53} - 8C_{55} + C_{56} + C_{57} - 2C_{59} + 4C_{78} + 8C_{87} - 4C_{88})\,, \\ b^{+-} &= -128\pi^4\ f_\pi^2\ (C_{56} + C_{57} - 2C_{59} - 4C_{78})\,. \end{aligned} \tag{3.39}$$

We have assumed the large-N_C limit to express the SU(2) definitions of the low-energy parameters $a_2^{00,+-}$ and $b^{00,+-}$ [75, 76] in terms of SU(3) chiral couplings. Taking into account these definitions, our relations simply predict:

$$\begin{aligned} a_2^{00} &= N_C^2\,, & b^{00} &= \frac{N_C^2}{6}\,, \\ a_2^{+-} &= 0\,, & b^{+-} &= 0. \end{aligned} \tag{3.40}$$

A simple explanation can be found for these results. From the previous discussion we know that there is no $a^n\pi\gamma$ interaction. One can also check that the $v^n\gamma\gamma$ interaction vanishes due to the special group structure from the $\langle f_+^{\mu\nu}\nabla_\mu v_\nu^n\rangle$ term. As a result, the only contribution to $\gamma\gamma \to \pi^0\pi^0$ at $\mathcal{O}(p^6)$ comes from the vector resonance exchanges in the crossed channels with two odd vertices, which turns out to be universal, i.e., independent of the 5D background. For $\gamma\gamma \to \pi^+\pi^-$ even this kind of diagram does not exist, so that a_2^{+-} and b^{+-} vanish. It will be interesting to calculate the corresponding amplitudes, to see if these properties remain. More relations among the other constants seem to hold, and this requires further investigation.

In table 6 we list the numerical results in different models, and isolate the odd-sector contributions, which are not negligible for some LECs and are sometimes even dominant. The different models provide similar results, up to a variation of the order of $\pm 1{\cdot}10^{-3}\,\mathrm{GeV}^{-2}$. One must be aware that when we perform a tree-level estimate of the renormalized chiral couplings we cannot specify at what renormalization scale μ they correspond, and a deviation of that order of magnitude might occur as one has the running [5, 6]

$$\frac{dC_k}{d\ln\mu^2} = \frac{1}{32\pi^2}\left[2\Gamma_k^{(1)} + \Gamma_k^{(L)}(\mu)\right], \tag{3.41}$$

with $\left|\frac{1}{32\pi^2}\left[2\Gamma_k^{(1)} + \Gamma_k^{(L)}(\mu)\right]\right| \sim 1\cdot 10^{-3}\,\mathrm{GeV}^{-2}$ [5, 6].

JHEP11(2012)012

	Odd contrib.	flat	"Cosh"	Hard-wall	Sakai-Sugimoto
C_1	—	0.5	−0.3	−0.9	−1.9
C_3	—	0.1	0.3	0.4	0.7
C_4	—	0.6	0	−0.5	−1.2
C_{40}	—	−0.5	0.2	0.8	1.8
C_{42}	2.6	1.9	2.2	2.5	3.0
C_{44}	−5.2	−4.1	−5.5	−6.6	−8.7
C_{46}	−2.6	−2.8	−3.2	−3.5	−4.0
C_{47}	5.2	5.5	6.2	6.8	7.8
C_{48}	6.4	5.6	5.8	5.9	6.2
$C_{50}+C_{90}$	12.7	17.4	19.1	20.2	22.2
$C_{51}+C_{90}$	—	3.1	5.2	6.7	9.2
$C_{52}-C_{90}$	−6.4	−10.6	−11.6	−12.1	−13.1
$C_{53}-\frac{1}{2}C_{90}$	4.0	−5.6	−8.8	−10.5	−13.4
$C_{55}+\frac{1}{2}C_{90}$	4.0	13.5	16.7	18.4	21.3
$C_{56}-C_{90}$	−7.9	2.6	7.1	9.5	13.3
$C_{57}+2C_{90}$	—	13.4	17.2	19.2	22.8
$C_{59}-\frac{1}{2}C_{90}$	−4.0	−16.0	−20.1	−22.3	−26.0
C_{66}	—	0.4	−0.3	−0.7	−1.5
C_{69}	—	−0.4	0.3	0.7	1.5
$C_{70}-\frac{1}{2}C_{90}$	0.3	2.8	5.3	6.9	9.6
$C_{72}+\frac{1}{2}C_{90}$	0.3	−2.9	−4.7	−5.9	−7.8
$C_{73}+C_{90}$	-0.5	-2.0	-4.4	-6.0	-8.7
C_{74}	—	−17.1	−19.0	−19.5	−20.4
$C_{76}-\frac{1}{2}C_{90}$	−0.3	8.5	11.1	12.7	15.3
$C_{78}+\frac{1}{2}C_{90}$	—	12.0	16.1	18.3	22.0
$C_{79}-\frac{1}{2}C_{90}$	—	2.8	4.1	4.8	6.0
C_{87}	—	4.9	6.8	7.7	9.3
$C_{88}-C_{90}$	—	−4.2	−5.2	−5.8	−6.7
C_{89}	—	22.6	29.2	32.7	38.8
C_{92}	—	42.4	68.8	87.3	171.0
C_{93}	—	−10.6	−17.2	−21.8	−42.8

Table 6. Numerical results for the $\mathcal{O}(p^6)$ low-energy constants of the even sector from different holographic models. All the results are in units of 10^{-3} GeV^{-2}. In the second column we provide the contribution from the odd-parity resonance sector.

In tables 7, 8 and 9 we compare our results from the "Cosh" model with the outcomes from other frameworks. In general, the different works constrain particular combinations of LECs through the analysis of various matrix elements. Some determinations consider the $\mathcal{O}(p^6)$ determination of the amplitudes and extract the couplings directly from the experimental data: $\pi\pi$ and πK scattering [11, 77], $\pi\pi$ VFF [78] an the $VV-AA$ correlator [9, 10]. Many authors were able to compute these LECs through rational approximants [12, 14],

JHEP11(2012)012

	"Cosh"	DSE [17]	$\mathcal{O}(p^6)$ χPT	Reson. Lagr. & Rational App.
$(-4C_1+8C_2$ $+5C_3+7C_4)$	2.6	$6.29^{+0.28}_{-0.42}$	10.1 ± 2.6 [77]	7.2 [77]
				5.9 ± 3.3 [59, 85]
				7.3 [6, 84]
$(3C_3+C_4)$	0.9	$2.95^{+0.11}_{-0.19}$	2.6 ± 0.3 [77]	2.0 [77]
			0.99 ± 0.25 [11]	1.00 [11]
			2.10 ± 0.25 [11]	1.7 ± 0.3 [59, 85]
			2.35 ± 0.23 [11]	2.0 [84]
(C_1+4C_3)	0.9	$3.59^{+0.13}_{-0.21}$	2.07 ± 0.49 [11]	0.72 [11]
			2.81 ± 0.49 [11]	
C_2	0	$0.00^{+0.13}_{-0.00}$	-0.92 ± 0.49 [11]	-0.05 [11]
			-0.74 ± 0.49 [11]	
$(C_1+2C_2+4C_3)$	0.9	$3.59^{+0.13}_{-0.21}$	0.23 ± 1.08 [11]	0.62 [11]
			1.34 ± 1.08 [11]	
$\pi\pi$, πK scattering			1.88 ± 0.72 [11]	
$(C_{88}-C_{90})$	-5.2	$-7.91^{-0.35}_{+0.57}$	-7.3 ± 0.5 [78]	-6.1 ± 0.5 [87]
				-8.6 [6, 78]
				-5.2 [82]
				-6.9 [81]
				-6.5 [81]
				-8.6 [81]
$\gamma \to \pi\pi$ form factor				-6.2 ± 0.6 [14]
$(2C_{78}-4C_{87}+C_{88})$	0	$-0.73^{-0.17}_{+0.25}$		2.5 [82]
				3.6 [6, 88]
				2.3 ± 8.4 [69]
				0.8 [81]
				1.8 [81]
$\pi, K \to \ell\nu\gamma$ form factor				3.2 [81]

Table 7. Comparison of our results from the the "Cosh" model for some particular combinations of the $\mathcal{O}(p^6)$ LECs in the even sector, with those from other approaches. All the results are in units of 10^{-3} GeV^{-2}. The χPT and resonance determinations [6, 59, 77, 84, 85] of $(-4C_1+8C_2+5C_3+7C_4)$ stem from the SU(2) combination of couplings r_5 under the assumption that the loop correction — $1/N_C$ suppressed — is neglected in the relation between SU(3) and SU(2) couplings at large N_C. A similar argument applies for the determinations [59, 77, 84, 85] for $(3C_3+C_4)$, which derives from the SU(2) parameter r_6.

large-N_C resonance estimates [6, 11, 16, 59, 69, 72, 73, 75–77, 79–85] and resonance determinations at NLO in the $1/N_C$ expansion [86, 87]. For the study [82] of the VAP, the $VV-AA$, the $SS-PP$ Green's functions and the scalar and vector form factors in RχT, we have used the inputs $m_\rho = 0.776\,\text{GeV}$, $m_{a_1} = 1.26\,\text{GeV}$, $m_{\pi'} = 1.3\,\text{GeV}$. Conversely, the analysis through the Dyson-Schwinger equation [17] is able to determine all the LECs (table 9).

JHEP11(2012)012

	"Cosh"	DSE [17]	$\mathcal{O}(p^6)$ χPT	Reson. Lagr. & Rational App.
$(8C_{53}+8C_{55}$ $+C_{56}+C_{57}+2C_{59})$	47.7	$20.7^{+0.2}_{-0.3}$		69 ± 19 [75, 80]
$(C_{56}+C_{57}+2C_{59})$	-15.9	$-17.7^{+0.6}_{-1.0}$		-32 ± 11 [75, 80]
$(8C_{53}-8C_{55}+C_{56}$ $+C_{57}-2C_{59}+4C_{78}$ $+8C_{87}-4C_{88})$	0	$-5.52^{-0.40}_{+0.67}$		3.7 [76]
$(C_{56}+C_{57}$ $-2C_{59}-4C_{78})$	0	$2.20^{+0.20}_{-0.25}$		-4.2 [76]
$\gamma\gamma \to \pi\pi$ **scattering**				
C_{87}	6.8	$7.57^{+0.37}_{-0.60}$	4.9 ± 0.2 [9, 10]	4.8 ± 1.3 [69] 4.0 [82] 7.6 [79] 5.3 [81] 6.2 [81] 8.6 [81] 4.1 ± 1.5 [86] 5.7 ± 0.5 [12]
$VV-AA$ **correlator**				
$\left(C_{78}+\frac{1}{2}C_{90}\right)$	16.1	$18.73^{+0.83}_{-1.36}$		11.8 [82] 14.4 [81] 16.6 [81] 23.1 [81]
C_{89}	29.2	$34.74^{+1.61}_{-2.62}$		19.6 [82] 26.0 [81] 30.3 [81] 42.5 [81]
C_{93}	-17.2			-8.4 [16, 72, 73] -17 [79]

Table 8. Comparison of our results from the the "Cosh" model for some particular combinations of the $\mathcal{O}(p^6)$ LECs in the even sector, with those from other approaches. All the results are in units of 10^{-3} GeV^{-2}. The $\gamma\gamma \to \pi\pi$ determinations [75, 76, 80], based on resonance estimates, were extracted from the SU(2) parameters a_2^r and b^r under the assumption that the ($1/N_C$ suppressed) loop corrections are neglected in the relation between SU(2) and SU(3) couplings at large N_C.

In tables 7 and 8 we show the results for particular combinations of the LECs that contribute directly to some processes. Here, some of these estimates have been extracted from SU(2) analyses [6, 59, 75–77, 80, 84, 85] under the assumption that the $1/N_C$-suppressed loop corrections are neglected in the relation between the SU(3) and SU(2) LECs at large N_C. One can see that some of the couplings ($C_{88}-C_{90}$, $2C_{78}-4C_{87}+C_{88}$, C_{87}, $C_{78}+\frac{1}{2}C_{90}$, C_{89}, C_{93}) are in relatively fair agreement. These are related with amplitudes with a small

JHEP11(2012)012

	"Cosh"	DSE [17]
C_1	-0.3	$3.79^{+0.10}_{-0.17}$
C_3	0.3	$-0.05^{+0.01}_{-0.01}$
C_4	0	$3.1^{+0.09}_{-0.15}$
C_{40}	0.2	$-6.35^{-0.18}_{+0.32}$
C_{42}	2.2	$0.60^{+0.00}_{-0.00}$
C_{44}	-5.5	$6.32^{+0.20}_{-0.36}$
C_{46}	-3.2	$-0.60^{-0.02}_{+0.04}$
C_{47}	6.2	$0.08^{+0.01}_{-0.00}$
C_{48}	5.8	$3.41^{+0.06}_{-0.10}$
$C_{50}+C_{90}$	19.1	$11.15^{+0.40}_{-0.66}$
$C_{51}+C_{90}$	5.2	$-9.05^{-0.20}_{+0.37}$
$C_{52}-C_{90}$	-11.6	$-7.48^{-0.29}_{+0.47}$
$C_{53}-\frac{1}{2}C_{90}$	-8.8	$-13.21^{-0.68}_{+1.10}$
$C_{55}+\frac{1}{2}C_{90}$	16.7	$18.01^{+0.77}_{-1.26}$
$C_{56}-C_{90}$	7.1	$16.90^{+0.90}_{-1.44}$
$C_{57}+2C_{90}$	17.2	$12.80^{+0.58}_{-0.93}$
$C_{59}-\frac{1}{2}C_{90}$	-20.1	$-23.71^{-1.02}_{+1.66}$
C_{66}	-0.3	$1.7^{+0.07}_{-0.12}$
C_{69}	0.3	$-0.86^{-0.04}_{+0.06}$
$C_{70}-\frac{1}{2}C_{90}$	5.3	$0.51^{+0.11}_{-0.16}$
$C_{72}+\frac{1}{2}C_{90}$	-4.7	$-2.08^{-0.14}_{+0.23}$
$C_{73}+C_{90}$	-4.4	$2.94^{+0.05}_{-0.10}$
C_{74}	-19.0	$-5.07^{-0.16}_{+0.27}$
$C_{76}-\frac{1}{2}C_{90}$	11.1	$-2.66^{-0.04}_{+0.08}$
$C_{78}+\frac{1}{2}C_{90}$	16.1	$18.73^{+0.83}_{-1.36}$
$C_{79}-\frac{1}{2}C_{90}$	4.1	$-1.78^{-0.11}_{+0.17}$
C_{87}	6.8	$7.6^{+0.4}_{-0.6}$
$C_{88}-C_{90}$	-5.2	$-7.91^{-0.35}_{+0.57}$
C_{89}	29.2	$34.7^{+1.6}_{-2.6}$
C_{92}	68.8	—
C_{93}	-17.2	—

Table 9. Comparison of our results for $\mathcal{O}(p^6)$ LECs of the even sector from the "Cosh" model and those from DSE [17]. The chiral couplings are in units of $10^{-3}\,\mathrm{GeV}^{-2}$.

number of external legs, which might be dominated by the lightest vector and axial-vector mesons. For those related to the $\pi\pi \to \pi\pi$ and $\gamma\gamma \to \pi\pi$ scattering, the agreement is a little worse, but still reasonable taking into account possible sub-leading differences between the physical and the large-N_C values of the chiral couplings.

In table 9 we compare our results for individual LECs from the "Cosh" model to those from the DSE approach [17]. For most couplings one finds a reasonable agreement, although

JHEP11(2012)012

for a few others there are larger deviations. In some cases, the discrepancy can be attributed to the odd-odd contributions mentioned before. Adding these contributions to the results from the DSE approach, many couplings, e.g., C_{42}, C_{46}, C_{47}, C_{52}, C_{53} and C_{56}, agree much better with ours. Some of the others are pushed towards our results, like C_{44} and C_{50}. Still, there are large differences for a few couplings, the most serious ones being C_{51}, C_{74} and C_{76}.

There are other possible contributions that may be responsible of the deviations. First, one should keep in mind that the present models include only the spin-1 resonance contributions, and that scalar mesons may play an important role in scattering processes. Second, our effective holographic action in principle could also accommodate operators of even higher dimension, e.g., of the type $(\mathcal{F}_{MN})^3$, that would modify the LECs related to processes with a larger number of external legs. These higher dimensional terms can appear from the low energy expansion of the Dirac-Born-Infeld (DBI) action [89, 90], and are companied by factors of α'. Since the α' expansion on the string side corresponds to the large λ expansion on the gauge theory side [91], the contributions from these operators will be suppressed when the 't Hooft coupling λ is very large. However, they could give corrections when this constraint is relaxed.

4 Relations between odd and even amplitudes

4.1 Green's function relation: the LR versus the VVA correlator

The relations between the anomalous $\mathcal{O}(p^6)$ constants and the $\mathcal{O}(p^4)$ constants in the even sector indicate possible relations between correlation functions or form factors in this class of models. One example is the Son-Yamamoto relation between the transverse triangle structure function $w_T(Q^2)$ and the left-right correlator [29]. Explicitly, $w_T(Q^2)$ is defined as the transverse part of the correlation function of the vector current and the axial current in a weak electromagnetic background field $\hat{F}_{\mu\nu}$:

$$i\int \mathrm{d}^4x\, e^{iqx}\langle j_\mu^a(x) j_\nu^{5b}(0)\rangle_{\hat{F}} = \frac{Q^2}{8\pi^2} d^{ab} P_\mu^{\alpha\perp}\left[P_\nu^{\beta\perp} w_T(q^2) + P_\nu^{\beta\parallel} w_L(q^2)\right]\epsilon_{\alpha\beta\sigma\rho}\hat{F}^{\sigma\rho}, \tag{4.1}$$

where $Q^2 = -q^2$, a and b are flavor indices and $d^{ab} = (1/2)\mathrm{tr}(\mathcal{Q}\{t^a, t^b\})$ with $\mathcal{Q}$ being the electric charge matrix, and $P_\mu^{\alpha\perp} = \eta_\mu^\alpha - q_\mu q^\alpha/q^2$ and $P_\mu^{\alpha\parallel} = q_\mu q^\alpha/q^2$ are the transverse and longitudinal projection tensors.

With the bulk-to-boundary propagators introduced before, w_T, Π_V and Π_A can be expressed in the holographic models as

$$w_T(Q^2) = \frac{N_C}{Q^2}\int_{-z_0}^{z_0} \mathrm{d}z A(Q,z)\partial_z V(Q,z) \tag{4.2}$$

$$\Pi_V(Q^2) = \frac{1}{Q^2} f^2(z) V(Q,z)\partial_z V(Q,z)|_{z=-z_0}^{z=+z_0} \tag{4.3}$$

$$\Pi_A(Q^2) = \frac{1}{Q^2} f^2(z) A(Q,z)\partial_z A(Q,z)|_{z=-z_0}^{z=+z_0}. \tag{4.4}$$

JHEP11(2012)012

Taking into account that $V(Q,z)$ and $A(Q,z)$ are two independent solutions of eq. (2.8) with different boundary conditions, one obtains the relation [29]

$$w_T(Q^2) = \frac{N_C}{Q^2} + \frac{N_C}{f_\pi^2}\left[\Pi_V(Q^2) - \Pi_A(Q^2)\right]. \tag{4.5}$$

Taking the $Q^2 \to 0$ limit on both sides, one gets the relation between C_{22}^W and L_{10} consistent with our result (3.27). Recent studies concerning the inclusion of the power corrections to the relation can be found in refs. [31, 32, 34–36].

4.2 Form factor relation: $\gamma^* \to \pi\pi$ versus $\pi^0 \to \gamma\gamma^*$

Now let us study more the relation (3.27) between C_{22}^W and L_9. Since C_{22}^W is also related to the anomalous $\pi\gamma^*\gamma^*$ form factor [92] and L_9 to the vector form factor of the pion [4], it is natural to ask if there is some relation between these two form factors. Actually, it has been pointed out that in two specific models they are equal up to normalization [41, 42]. We show that the relation is universal in the class of models considered here. The vector form factor $F_\pi(Q^2)$ is defined as

$$\langle \pi^+(p_1)|j_\mu^{\rm EM}(0)|\pi^+(p_2)\rangle = \mathcal{F}_\pi(Q^2)(p_1+p_2)_\mu\,, \tag{4.6}$$

with $j_\mu^{\rm EM} = \bar{q}\gamma_\mu \mathcal{Q} q$ the electromagnetic current ($\mathcal{Q}$ the charge operator), and $Q^2 = -(p_2 - p_1)^2$. Holographically, it has been derived in ref. [24] (see also [41]), and in our notation is given by

$$\begin{aligned}\mathcal{F}_\pi(Q^2) &= 1 - \frac{Q^2}{2f_\pi^2}\int_{-z_0}^{z_0}\frac{1}{g^2(z)}V(Q,z)(1-\psi_0^2)\mathrm{d}z \\ &= \frac{1}{f_\pi^2}\int_{-z_0}^{z_0} f^2(z)V(Q,z)\psi_0'(z)^2\mathrm{d}z.\end{aligned} \tag{4.7}$$

The anomalous $\pi\gamma^*\gamma^*$ form factor is defined by

$$\begin{aligned}&\int d^4x\; e^{-iq_1x}\langle \pi, p|T\left\{J_{\rm EM}^\mu(x)\,J_{\rm EM}^\nu(0)\right\}|0\rangle \\ &\qquad = \epsilon^{\mu\nu\alpha\beta} q_{1\,\alpha} q_{2\,\beta}\,\mathcal{F}_{\gamma^*\gamma^*\pi^0}\left(Q_1^2, Q_2^2\right)\,,\end{aligned} \tag{4.8}$$

where q_1, q_2 are the momenta of photons, and $q_{1,2}^2 = -Q_{1,2}^2$. For real photons

$$\mathcal{F}_{\gamma^*\gamma^*\pi^0}(0,0) = \frac{N_C}{12\pi^2 f_\pi} \tag{4.9}$$

reproduces the anomaly in QCD. From the holographic approach, the form factor was derived in ref. [41] in the hard wall, and the expression for a general background is

$$\mathcal{F}_{\gamma^*\gamma^*\pi}(Q_1^2, Q_2^2) = \frac{N_C}{24\pi^2 f_\pi}\int_{-z_0}^{z_0} V(Q_1,z)V(Q_2,z)\psi_0'(z)\mathrm{d}z. \tag{4.10}$$

Taking the limit $Q_1^2 = Q_2^2 = 0$ one recovers the value in eq. (4.9). As shown in ref. [41], this confirms the choice of the coefficient of the CS term in the action. Employing the equation of motion for $\psi_0(z)$, one finds

$$\mathcal{F}_{\gamma^*\gamma^*\pi}(Q^2, 0) = \frac{N_C}{12\pi^2 f_\pi}\,\mathcal{F}_\pi(Q^2). \tag{4.11}$$

JHEP11(2012)012

Taking the slope at $Q^2 = 0$ on both sides, one obtains the relation between C_{22}^W and L_9 in eq. (3.27).

In the previous section we have shown that the results for the LECs do not sensibly depend on the details of the different models. However, for the form factors, the results from different models can differ from each other, especially in the high momentum region. Depending on the asymptotic metric in the UV, the form factor exhibits different power behavior when $Q^2 \to \infty$. For $\mathcal{F}_{\gamma^*\gamma^*\pi}(Q^2, 0)$, the explicit high-energy power structure in different models is analyzed in ref. [93]. In figure 2 and figure 3 we show the numerical results of both the form factors in the relation (4.11) for the four different models, together with the available experimental data.[2] From the figures one clearly finds the different power behavior of each model. To reproduce the observed $1/Q^2$ behavior for the form factors, the models need to be asymptotically AdS in the UV, and this is the case of the "Cosh" and hard wall models. In such models, one can simplify the metric functions in the UV region by using the Poincaré coordinates

$$f^2(u) = 1/g^2(u) \sim 1/g_5^2 u, \quad u \to 0. \tag{4.12}$$

Following the procedure in ref. [103], one finds the large-Q^2 behavior of the form factors [41]

$$\mathcal{F}_\pi(Q^2) \to \frac{f_\pi^2 g_5^2}{Q^2}, \qquad \mathcal{F}_{\gamma^*\gamma^*\pi}(Q^2, 0) \to \frac{N_C g_5^2 f_\pi}{12\pi^2 Q^2}. \tag{4.13}$$

The relation (4.11) between the two form factors dictates that the leading-power coefficients are proportional to each other. However, new experimental data for the vector form factor in the large momentum region are needed to confirm this. It is worth mentioning that, if the 5D coupling g_5 is fixed through the comparison with the perturbative logarithmic term of the vector correlator, $g_5^2 = 24\pi^2/N_C$ [19], then the above asymptotic behavior of $\mathcal{F}_{\gamma^*\gamma^*\pi}(Q^2, 0)$ is the same as the perturbative result [104–106]. With this, the vector form factor has the high energy behavior $Q^2\mathcal{F}_\pi(Q^2) \to 8\pi^2 f_\pi^2$ [41].

4.3 Form factor relation: $A \to \pi\pi\pi$ versus $\pi \to AA$

One may speculate whether there is a similar relation between the form factors involving the axial-vector source, based on eq. (3.28). In addition to the one-resonance terms (3.2) and (3.3), we need the operators with two resonance fields:

$$\begin{aligned} S_{YM}\Big|_{2-\text{res.}} &= i\, c_{a^m v^n \pi} \int d^4x \,\langle\, (\nabla_\mu v_\nu^n - \nabla_\nu v_\mu^n)\,[u^\mu, a^{m\,\nu}] + (\nabla_\mu a_\nu^m - \nabla_\nu a_\mu^m)\,[u^\mu, v^{n\,\nu}] \,\rangle + \dots \\ S_{CS}\Big|_{2-\text{res.}} &= \frac{N_C}{6\pi^2}\, \tilde{c}_{a^n a^m}\, \epsilon^{\mu\nu\alpha\beta} \int d^4x \,\langle\, u_\mu \{a_\nu^n, \nabla_\alpha a_\beta^m\} \,\rangle \quad + \quad \dots \end{aligned} \tag{4.14}$$

where the dots stand for operators which are not relevant for the calculation of the $\pi \to AA$ and $A \to \pi\pi\pi$ form factors. The resonance couplings are given by the 5D integrals

$$\begin{aligned} c_{a^m v^n \pi} &= \int_{-z_0}^{z_0} dz\, \frac{1}{g^2(z)}\, \psi_0(z)\, \psi_{2m}(z) \psi_{2n-1}(z)\,, \\ \tilde{c}_{a^n a^m} &= \int_{-z_0}^{z_0} dz\, \psi_0(z)\, \psi_{2n}(z)\, \psi'_{2m}(z)\,, \end{aligned} \tag{4.15}$$

A detailed calculation of the resonance couplings from the CS term can be found in ref. [112].

[2] For a review and references of the $\pi\gamma^*\gamma^*$ form factor, please see ref. [94–102].

JHEP11(2012)012

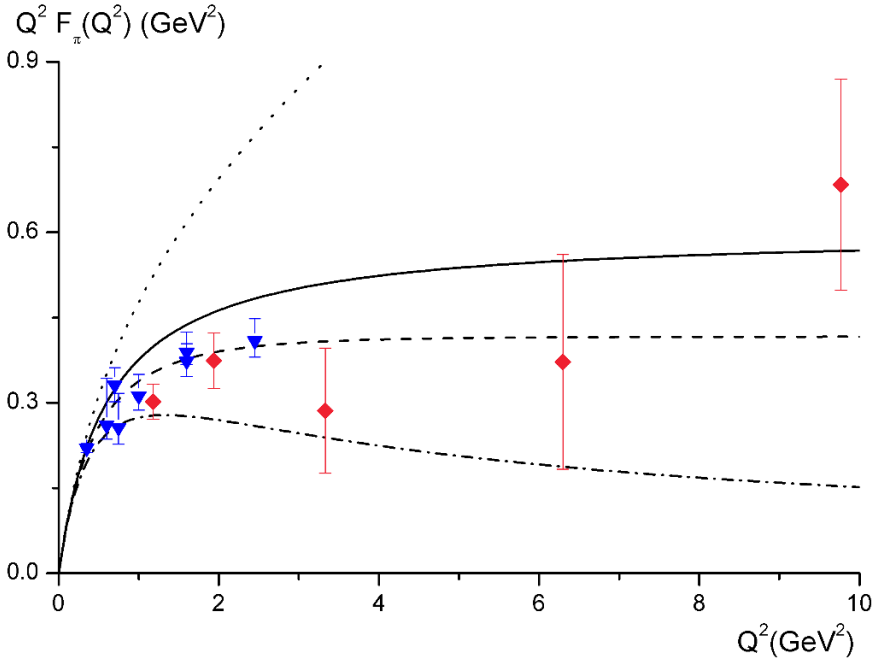

Figure 2. Vector form factor $\mathcal{F}_\pi(Q^2)$ from the flat, "Cosh", hard wall and Sakai-Sugimoto models, denoted by the dotted, solid, dashed and dash-dotted lines, respectively. The experimental data are from ref. [107] (diamonds) and ref. [108] (triangles).

4.3.1 Odd-sector form factor: $\pi \to AA$

In parallel with the pion-photon transition form factor, we can relate C_{23}^W to the form factor involving two axial-vector sources:

$$\begin{aligned}\int &< \pi^c(p)|T\{j_\mu^{5a}(x) j_\nu^{5b}(0)\}|0> e^{-iq_1 x} \mathrm{d}^4x \\ &= \frac{i\ N_C}{24\pi^2 f_\pi}\ D^{abc}\ \epsilon_{\mu\nu\alpha\beta}\ q_1^\alpha q_2^\beta\ \mathcal{F}_{\pi AA}(Q_1^2, Q_2^2),\end{aligned} \tag{4.16}$$

with $p = q_1 + q_2$, $Q_1^2 = -q_1^2$, $Q_2^2 = -q_2^2$. Here we are considering the axial current $j_\mu^{5a} = \bar{q}\gamma_\mu\gamma_5 t^a q$ with t^a the generator in $\mathrm{U}(N_f)$, $D^{abc} = 2\mathrm{Tr}(\{t^a, t^b\}t^c)$ is the corresponding fully symmetric tensor. At low-energies, this form factor is given in χPT by the expression

$$\mathcal{F}_{\pi AA}(Q_1^2, Q_2^2) = 1 + \frac{192\pi^2 C_{23}^W}{N_C}(Q_1^2 + Q_2^2) \quad + \ \mathcal{O}(E^4)\,, \tag{4.17}$$

where higher order corrections are in the $\mathcal{O}(E^4)$ term. Computing the local diagrams from the WZW term and the one and two axial-vector resonance exchanges one gets:

$$\begin{aligned}\mathcal{F}_{\pi AA}(Q_1^2, Q_2^2) = 1 &- \sum_n \frac{3 a_{Aa^n} c_{a^n}}{2}\left[\frac{Q_1^2}{m_{a^n}^2 + Q_1^2} + \frac{Q_2^2}{m_{a^n}^2 + Q_2^2}\right] \\ &+ \sum_{m,n} \frac{3 c_{a^n a^m} a_{Aa^n} Q_1^2}{(m_{a^n}^2 + Q_1^2)} \frac{a_{Aa^m} Q_2^2}{(m_{a^m}^2 + Q_2^2)}\,.\end{aligned} \tag{4.18}$$

JHEP11(2012)012

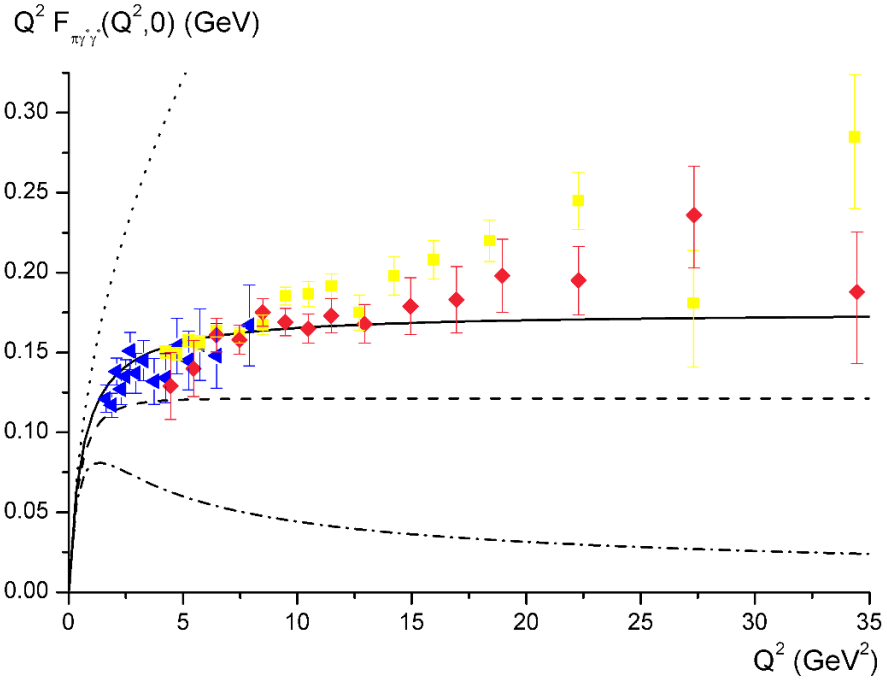

Figure 3. Anomalous $\pi\gamma^*\gamma^*$ form factor from the flat, "Cosh", hard wall and Sakai-Sugimoto models, with the same notation as in figure 2. The experimental data are from CLEO [109] (triangles), BABAR [110] (squares) and BELLE collaboration [111] (diamonds).

where $c_{a^n a^m} = -\frac{1}{2}\tilde{c}_{a^n a^m} - \frac{1}{2}\tilde{c}_{a^m a^n}$. If one sets to zero the squared momentum of one of the axial-vector sources, the $\pi \to AA$ form factor becomes

$$\mathcal{F}_{\pi AA}(Q^2, 0) = 1 - \sum_n \frac{3 a_{A a^n} c_{a^n}}{2} \frac{Q^2}{m_{a^n}^2 + Q^2} \,. \tag{4.19}$$

In the holographic approach, following the same procedure as the $\pi\gamma^*\gamma^*$ form factor, we can express this form factor through the bulk-to-boundary propagator $A(Q, z)$

$$\mathcal{F}_{\pi AA}(Q_1^2, Q_2^2) = \frac{3}{2} \int_{-z_0}^{z_0} A(Q_1, z) A(Q_2, z) \psi_0'(z) \mathrm{d}z. \tag{4.20}$$

4.3.2 Even-sector form factor: $A \to \pi\pi\pi$

In the YM part, in parallel with the vector form factor, we can define the form factor involving an axial-vector source and three pions

$$\begin{aligned} &< \pi^a(p_1)\pi^b(p_2)\pi^c(p_3)|ij_\mu^{5d}|0> \\ &= f^{bce} f^{ade}\ P_\mu^{\nu\perp}(q)[\mathcal{F}_1(Q^2, s, t)(p_1 - p_3)_\nu + \mathcal{F}_2(Q^2, s, t)(p_2 - p_3)_\nu] + (a \leftrightarrow c), \end{aligned} \tag{4.21}$$

where $q = p_1 + p_2 + p_3$, $P_\alpha^{\mu\perp}(q) = \eta_\alpha^\mu - q_\alpha q^\mu / q^2$, $Q^2 = -q^2$, $s = (p_1 + p_3)^2$, $t = (p_2 + p_3)^2$, and we also use $u = (p_1 + p_2)^2$, which obeys the Mandelstam relation $s + t + u = q^2$ (the light

JHEP11(2012)012

pseudo-scalars are massless in the chiral limit considered all along this article). Due to Bose symmetry, the two form factors $\mathcal{F}_1$ and $\mathcal{F}_2$ are related through $\mathcal{F}_1(Q^2,s,t)=\mathcal{F}_2(Q^2,t,s)$. At large distances, χPT yields the amplitude

$$\mathcal{F}_1(Q^2,s,t)=\frac{2}{3f_\pi}\left[1\;+\;\frac{2L_9\,q^2}{f_\pi^2}\;-\;\frac{16L_1(u+t-s/2)}{f_\pi^2}\;+\;\mathcal{O}(E^4)\right]. \tag{4.22}$$

In the limit $s,t\to 0$ (i.e., $p_3^\mu\to 0$), hence $u\to q^2$, this expression becomes:

$$\mathcal{F}_1(Q^2,0,0)=\frac{2}{3f_\pi}\left[1\;+\;\frac{2q^2\,(L_9-8L_1)}{f_\pi^2}\;+\;\mathcal{O}(q^4)\right]. \tag{4.23}$$

The extraction of the form factor through the 5D action turns out to be difficult. Instead, we choose to work in the 4D picture and include all the contributions diagram by diagram. Summing up the diagrams with only Goldstones, one-resonance and two-resonance exchanges, we obtain:

$$\begin{aligned}\mathcal{F}_1(Q^2,s,t)=\frac{2}{3f_\pi}\Bigg\{1\;+\;&\frac{2L_9\,q^2}{f_\pi^2}\;-\;\frac{16L_1(u+t-s/2)}{f_\pi^2}+\sum_n\frac{a_{Aa^n}b_{a^n\pi^3}}{2f_\pi^2}\,\frac{q^2(u+t-s/2)}{m_{a^n}^2-q^2}\\&+\sum_n\Bigg[\frac{(a_{Vv^n}-b_{v^n\pi\pi})b_{v^n\pi\pi}}{4f_\pi^2}\left(\frac{(2u-t)s}{m_{v^n}^2-s}\;-\;\frac{(u-s)t}{m_{v^n}^2-t}\right)\\&\qquad+\frac{a_{Vv^n}b_{v^n\pi\pi}}{4f_\pi^2}\left(\frac{(6s+u+2t)s}{m_{v^n}^2-s}\;-\;\frac{(s-u)t}{m_{v^n}^2-t}\right)\;-\;\frac{3b_{v^n\pi\pi}^2}{8f_\pi^2}\,\frac{(u+t)s}{m_{v^n}^2-s}\Bigg]\\&+\sum_{m,n}\frac{a_{Aa^m}c_{a^mv^n\pi}b_{v^n\pi\pi}}{4f_\pi^2}\,\frac{q^2}{m_{a^m}^2-q^2}\left(\frac{s(2u+t)}{m_{v^n}^2-s}+\frac{t(s-u)}{m_{v^n}^2-t}\right)\Bigg\}.\end{aligned} \tag{4.24}$$

In the kinematic configuration $s=t=0$ the contribution from diagrams where two of the Goldstones are produced through an intermediate vector resonance vanishes. Thus, the form factor is greatly simplified into

$$\mathcal{F}_1(Q^2,0,0)=\frac{2}{3f_\pi}\left[1\;+\;\frac{2q^2\,(L_9-8L_1)}{f_\pi^2}+\sum_n\frac{a_{Aa^n}b_{a^n\pi^3}}{2f_\pi^2}\,\frac{q^4}{m_{a^n}^2-q^2}\right]. \tag{4.25}$$

It is interesting to observe that, in the case when the resonance summations in the sum rules in eq. (3.11) are convergent, the dominant high-energy power behavior is given by

$$\begin{aligned}\mathcal{F}_1(Q^2,0,0)=\frac{2}{3f_\pi}\Bigg[\;&\frac{q^2}{2f_\pi^2}\left(4L_9-32L_1\;-\;\sum_n a_{Aa^n}b_{a^n\pi^3}\right)\\&+\left(1-\sum_n\frac{a_{Aa^n}b_{a^n\pi^3}m_{a^n}^2}{2f_\pi^2}\right)\;+\;\dots\Bigg],\end{aligned} \tag{4.26}$$

where the dots stand for contributions that vanish at high energies. A closer look at the sum rules (3.11) leads to the prediction $\mathcal{F}_1(Q^2,0,0)\overset{q^2\to\infty}{\longrightarrow}0$. This short-distance condition can serve to further constrain the $A\to\pi\pi\pi$ amplitude in the case when only the lightest resonances are taken into account [39, 40].

JHEP11(2012)012

The form factor can be rewritten in terms of the bulk-to-boundary propagators and the Green's function $G(Q^2;z,z')$ provided in (2.18):

$$\begin{aligned}\mathcal{F}_1(Q^2,s,t) = &\frac{2}{3f_\pi}+\frac{1}{3f_\pi}(6s+3u+t)\frac{\mathcal{F}_\pi(-s)-1}{s}\\ &-\frac{2}{3f_\pi^3}L_9(3s+3u+t)+\frac{1}{3f_\pi^3}(u+t-s/2)\frac{\mathcal{F}_0(Q^2)}{Q^2}\\ &+\frac{1}{6f_\pi^3}(s-u)T_1(-t)-\frac{1}{18f_\pi^3}(8u-t)T_1(-s)-\frac{1}{3f_\pi^3}(s-u)T_2(Q^2,-t)\end{aligned} \tag{4.27}$$

with

$$\begin{aligned}\mathcal{F}_0(Q^2) &\equiv Q^2\int_{-z_0}^{z_0}\frac{\psi_0(1-\psi_0^2)}{g^2(z)}A(Q,z)\mathrm{d}z\\ T_1(-t) &\equiv \int_{-z_0}^{z_0}\int_{-z_0}^{z_0}\frac{1-\psi_0(z)^2}{g^2(z)}\frac{1-\psi_0(z')^2}{g^2(z')}\,tG(-t,z,z')\,\mathrm{d}z\mathrm{d}z'\\ T_2(Q^2,-t) &\equiv \int_{-z_0}^{z_0}\int_{-z_0}^{z_0}\frac{1-\psi_0(z)A(Q,z)}{g^2(z)}\frac{1-\psi_0(z')^2}{g^2(z')}\,tG(-t,z,z')\,\mathrm{d}z\mathrm{d}z',\end{aligned} \tag{4.28}$$

and $\mathcal{F}_\pi$ the vector form factor. Since the final result for the form factor involves only those 5D quantities, it seems possible to derive it directly from the original YM action: this is still under investigation. In the kinematical limit $s,t\to 0$ this expression becomes:

$$\mathcal{F}_1(Q^2,0,0) \;=\; \frac{2}{3f_\pi}\left[1-\frac{1}{2f_\pi^2}\mathcal{F}_0(Q^2)\right]. \tag{4.29}$$

4.3.3 Comparison of anomalous and even-sector form factors

By means of the equation of motion for the bulk-to-boundary propagator $A(Q,z)$, one can also express the anomalous form factor (4.20) in terms of the previously defined function $\mathcal{F}_0(Q^2)$. Hence, independently of the precise details of the models, one finds the relation:

$$\mathcal{F}_1(Q^2,0,0) \;=\; \frac{2}{3f_\pi}\,\mathcal{F}_{\pi AA}(Q^2,0)\,. \tag{4.30}$$

This constitutes the generalization of the relation $C_{23}^W = \frac{N_C}{96\pi^2 f_\pi^2}(L_9-8L_1)$ in eq. (3.28) between the odd-sector $\mathcal{O}(p^6)$ LEC C_{23}^W and the even-sector $\mathcal{O}(p^4)$ chiral couplings L_1 and L_9. Indeed, as a final check, if one studies (4.30) at low energies with the help of their χPT expansions (4.17) and (4.23), one recovers the relation (3.28). In figure 4 we show the numerical results of the form factor $\mathcal{F}_{\pi AA}(Q^2,0)$ in different models. One finds that the asymptotic behavior is similar to the corresponding one for the $\pi\gamma\gamma^*$ form factor.

From eqs. (3.18)–(3.26) one might speculate the possible existence of more relations of this kind between even and odd-sector amplitudes. This will be the subject of future studies.

5 Conclusions

We have performed an exhaustive study of the $\mathcal{O}(p^6)$ LECs for the 5D holographic theories which implement chiral symmetry breaking through different boundary conditions in the

JHEP11(2012)012

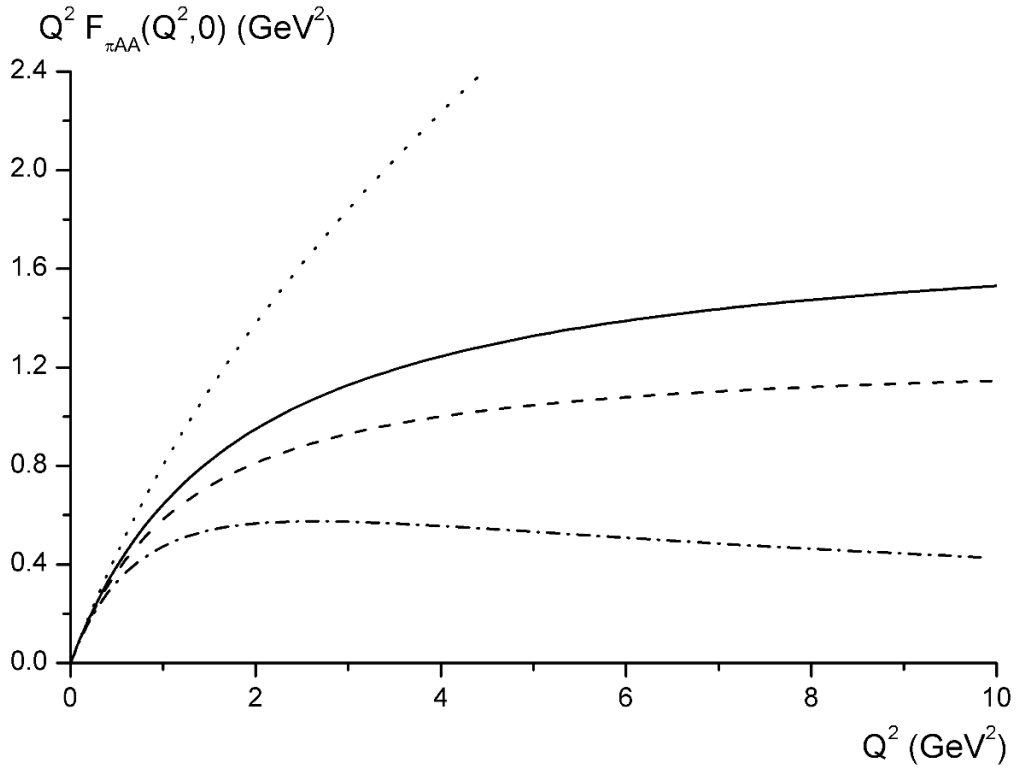

Figure 4. Results for the πAA transition form factor in the flat (dotted), "Cosh" (solid), hard wall (dashed) and Sakai-Sugimoto (dash-dotted) models.

infrared. The five-dimensional action was given by the Yang-Mills and the Chern-Simons terms. All the theoretical relations are determined for general backgrounds $f^2(z)$ and $g^2(z)$. Only for the numerical results we specified the precise expressions for such functions, which were taken from four models: "flat" background [19], "Cosh" model [19], hard-wall [24] and the Sakai-Sugimoto model [23, 25]. We found that the outcome for the LECs was stable, with a weak dependence on the background. We considered the results from the "Cosh" model as our best estimate, since this model, among the four studied ones, better matches the experimental $\rho(770)$ mass and pion decay constant in addition to the perturbative QCD log coefficient in the VV correlator. Remarkably, this model reproduces fairly well the new experimental data for the $\pi^0 \to \gamma\gamma^*$ transition form factor.

As a previous step, we worked out several resonance sum rules which became essential for the relations between the odd-parity and even LEC's derived later. Likewise, some of these sum rules were employed in the form factor analysis. For the sake of completeness, we derived (or rederived in some cases [24, 25]) all the sum rules we could, regardless of whether we used them in our later study. As many of these sum rules are used in hadronic phenomenology to fix the resonance parameters, we checked and found that, in general, the lowest meson exchanges provide the dominant contributions. The only exception was the sum rules related to the $VV - AA$ correlator, which are divergent due to the meson mass behavior $m^2_{R^n} \sim n^2$ in this kind of holographic models.

JHEP11(2012)012

We have computed the $\mathcal{O}(p^6)$ chiral couplings by integrating out the heavy resonances in the generating functional. In the odd-parity sector, we were able to express all the odd $\mathcal{O}(p^6)$ LECs in terms of even-sector $\mathcal{O}(p^4)$ couplings L_1 and L_9, and the 5D integral Z, which can be also defined from a sum rule. In particular, we recovered the LEC relation $C_{22}^W = -\frac{N_C}{32\pi^2 f_\pi^2} L_{10}$ [37] that stems from the Son-Yamamoto relation between the LR and AVV Green's functions [29]. These relations are general for the type of holographic theories considered here, and do not depend on the details of the functions $f^2(z)$ and $g^2(z)$ that specify the model. At the numerical level, the outcomes were found to be fairly stable, suffering little variation between the various holographic models studied here. Not much is known about the LECs of the odd-parity sector: we have compared our holographic determinations to those from other approaches (DSE, $\mathcal{O}(p^6)$ χPT phenomenological analyses, resonance estimates and rational approximations). In general we have found a reasonable agreement, considering that subleading $1/N_C$ corrections are not taken into account in the holographic approach and that there is an inherent uncertainty on the renormalization scale μ at which our large-N_C determinations correspond. We also tested a theoretical relation (3.29) derived from Resonance Chiral Theory [64], which was pretty well satisfied by the lightest resonance multiplets.

The $\mathcal{O}(p^6)$ even-parity LECs have also been determined. Since our framework does not include scalar-pseudoscalar sources χ, we obtained predictions only for the χPT operators without χ. Indeed, in the $\chi = 0$ limit the basis of $\mathcal{O}(p^6)$ operators in the chiral action can be further simplified, and we chose to eliminate the operator referred by C_{90}. We have also found some relations between $\mathcal{O}(p^6)$ couplings in the even-parity sector. In particular, those combinations of LECs related to the axial-vector form factor in the $P \to \ell\nu\gamma$ decay and to the $\gamma\gamma \to \pi\pi$ collision either vanish or can be expressed in terms of just f_π, independently of the holographic theory at hand. There is a wider phenomenology on the $\mathcal{O}(p^6)$ couplings of the even sector. Nonetheless, most of them remain essentially unknown. The agreement with former results (DSE, $\mathcal{O}(p^6)$ χPT determinations, resonance estimates and rational approximations) is reasonably good. Apart from a DSE analysis, which was able to provide the full set of LECs [17], there are no other approaches to compare most of our chiral coupling estimates with. The larger disagreements are found for the couplings that receive contributions from two odd-parity resonance couplings. Taking these contributions into account, one finds a better agreement with the corresponding DSE outcomes. In other few cases, the disagreement cannot be explained in this way, however, the corresponding couplings are related to processes with a high number of external legs. In string constructions, higher dimensional terms like $(\mathcal{F}_{MN})^3$ could appear from the low energy expansion of the DBI action. They would modify the value of those LECs if we do not insist that the 't Hooft coupling λ be very large. Likewise, scalar resonances are absent in our approach, and they may play a role in some LECs.

Some of the relations we have just found among couplings of different parity χPT Lagrangians are the consequence of relations between QCD amplitudes of the anomalous and even-parity sectors. The original motivation for this work was the relation found by Son and Yamamoto between the LR and AVV Green's functions [29]. We found that, for any type of background, the $\pi\pi$ vector form factor and the $\pi \to \gamma\gamma^*$ transition form factor

JHEP11(2012)012

are identical for any energy up to a known overall normalization, as it was already hinted in previous works [42, 103]. At large momentum, this relation dictates that the leading-power coefficients are proportional to each other, which can be experimentally checked. In the last section we studied the pion transition into two axial-vector currents and the axial-vector form factor into three pions. We found a relation between them for a particular kinematical configuration. In addition, we showed how this and the previous amplitudes could be rewritten from the 4D picture (with an infinite number of resonance exchanges) into a holographic form (in terms of bulk-to-boundary propagators). However, in the case of the $\pi\pi\pi$ AFF, with four external legs, one also needs to include the contributions with bulk-to-bulk Green's function propagators connecting two points in the bulk z and z'. All these amplitude relations, when taken to the low energy limit and compared at each chiral order, reproduce the relations between the odd and even-parity LECs we derived through the generating functional, serving as a double-check of our chiral coupling determinations.

The study of other consequences of some of the relations obtained here both in the odd and even sectors of QCD, e.g., those in the $P \to \ell\nu\gamma$ decay or the $\gamma\gamma \to \pi\pi$ scattering, requires new dedicated analyses. Moreover, new experimental data on the various form factors, in particular at high energies, would definitely help to discern the most appropriate version among the various holographic models, in the search of a precise dual formulation of QCD.

Acknowledgments

We thank F. De Fazio, F. Giannuzzi, L. Girlanda, K. Kampf and S. Nicotri for their comments on the paper and discussions. We are also grateful to S. Peris and A. Vainshtein for comments about the validity of the Son-Yamamoto relation in SU(3), and Qing Wang for explaining the anomaly structure in the Dyson-Schwinger equation approach. This work is partially supported by the Italian MIUR PRIN 2009. J.J.S.C. has been partially supported by the Universidad CEU Cardenal Herrera grants PRCEU-UCH15/10 and PRCEU-UCH35/11, and the MICINN-INFN fund AIC-D-2011-0818. F.Z. was supported in part by the National Natural Science Foundation of China under Grant No. 11135011.

A Holographic models

Four different holographic models have been studied in the present paper, among them the "Cosh" and "hard wall" background are asymptotically AdS in the UV. In all these models there are two parameters, the 5D gauge coupling g_5, and the energy scale Λ (or z_0^{-1}). We fix them in a unified way through the ρ meson mass $m_\rho = 0.776$ GeV and the pion decay constant $f_\pi = 0.087$ GeV. Therefore, the results for g_5 differ from that fixed through the high-energy vector correlator in asymptotically AdS models, which gives $g_5^2 = 24\pi^2/N_C$ [19]. In the non-AdS models, one is able to fix it in this way because the perturbative QCD logarithm is not recovered.

JHEP11(2012)012

A.1 "Flat" background

The model is specified by [19]

$$f^2(z) = \Lambda^2/g_5^2, \quad g^2(z) = g_5^2, \quad z_0 = 1. \tag{A.1}$$

The pion decay constant, meson masses, wave functions and couplings are given by

$$\begin{aligned}
V(Q,z) &= \frac{\cosh(Qz/\Lambda)}{\cosh(Q/\Lambda)}, & A(Q,z) &= \frac{\sinh(Qz/\Lambda)}{\sinh(Q/\Lambda)},\\
f_\pi^2 &= \frac{2\Lambda^2}{g_5^2}, & \psi_0(z) &= z,\\
m_n^2 &= \frac{\pi^2\Lambda^2}{4}n^2, & \psi_n(z) &= (-1)^{n-1}g_5 \sin\left(\frac{n\pi}{2}(z+1)\right),\\
a_{V^{v^n}} &= a_{2n-1}, \qquad a_{A^{a^n}} = a_{2n}, & a_n &= \frac{4}{n\pi g_5}\\
c_{v^n} &= \frac{2g_5}{(2n-1)\pi}, & c_{a^n} &= \frac{2g_5}{n\pi},\\
d_{v^n} &= \frac{2g_5}{(2n-1)\pi}\left[1 - \frac{8}{(2n-1)^2\pi^2}\right].
\end{aligned} \tag{A.2}$$

A.2 "Cosh" model

The background functions are specified by [19]

$$f^2(z) = \Lambda^2\cosh^2(z)/g_5^2, \quad g^2(z) = g_5^2, \quad z_0 = \infty. \tag{A.3}$$

The various solutions and physical quantities are

$$\begin{aligned}
V(Q,z) &= -\frac{\pi}{2}\csc(\nu\pi)\sqrt{1-\tanh^2 z}[P_\nu^1(\tanh z) + P_\nu^1(-\tanh z)],\\
A(Q,z) &= \frac{\pi}{2}\csc(\nu\pi)\sqrt{1-\tanh^2 z}[P_\nu^1(\tanh z) - P_\nu^1(-\tanh z)],\\
f_\pi^2 &= \frac{2\Lambda^2}{g_5^2}, & \psi_0(z) &= \tanh z,\\
m_n^2 &= n(n+1)\Lambda^2,\\
\psi_n(z) &= -g_5 c_n \frac{P_n^1(\tanh z)}{\cosh z}, & c_n &= \sqrt{\frac{2n+1}{2n(n+1)}},
\end{aligned} \tag{A.4}$$

$$\begin{aligned}
a_{V^{v^n}} &= a_{2n-1}, \qquad a_{A^{a^n}} = a_{2n}, \qquad a_n = \frac{1}{g_5}\sqrt{\frac{2(2n+1)}{n(n+1)}},\\
c_{v^n} &= \frac{g_5}{\sqrt{3}}\delta_{n,1}, \qquad c_{a^n} = \frac{2g_5}{\sqrt{15}}\delta_{n,1},\\
d_{v^n} &= \frac{\sqrt{3}g_5}{15}\delta_{n,1} + \frac{2\sqrt{42}g_5}{105}\delta_{n,2},
\end{aligned} \tag{A.5}$$

where $\nu(\nu+1) = -Q^2/\Lambda^2$, and $P_\nu^1(z)$ is the associate Legendre function.

JHEP11(2012)012

A.3 Hard-wall model

In this case the functions $f^2(z)$ and $g^2(z)$ are given by [24]

$$f^2(z) = \frac{1}{g_5^2(z_0 - |z|)}, \quad g^2(z) = g_5^2(z_0 - |z|), \quad z_0 < \infty. \tag{A.6}$$

It is more convenient to focus on the interval $0 < z < z_0$, and use the coordinate $\tilde{z} = z_0 - z$. Then we have:

$$\begin{aligned}
V(Q,\tilde{z}) &= Q\tilde{z}\left[K_1(Q\tilde{z}) + I_1(Q\tilde{z})\frac{K_0(Qz_0)}{I_0(Qz_0)}\right], \\
A(Q,\tilde{z}) &= Q\tilde{z}\left[K_1(Q\tilde{z}) - I_1(Q\tilde{z})\frac{K_1(Qz_0)}{I_1(Qz_0)}\right], \\
f_\pi^2 &= \frac{4}{g_5^2 z_0^2}, & \psi_0(\tilde{z}) &= 1 - \frac{\tilde{z}^2}{z_0^2}, \\
m_{v_n} &= \frac{\gamma_{0,n}}{z_0}, & m_{a_n} &= \frac{\gamma_{1,n}}{z_0}, \\
\psi_{v_n}(\tilde{z}) &= \frac{g_5}{z_0|J_1(\gamma_{0,n})|}\tilde{z}\; J_1\left(m_{v_n}\tilde{z}\right), \\
\psi_{a_n}(\tilde{z}) &= \frac{g_5}{z_0\left[-J_0(\gamma_{1,n})J_2(\gamma_{1,n})\right]^{1/2}}\tilde{z}\; J_1\left(m_{a_n}\tilde{z}\right).
\end{aligned} \tag{A.7}$$

Here $K_n(x)$, $I_n(x)$ and $J_n(x)$ are Bessel functions, and $\gamma_{n,m}$ is the m^{th} root of $J_n(x)$. The couplings $a_{Vv^n}, a_{Aa^n}, c_{v^n}, c_{a^n}, d_{v^n}$ can be calculated from these wave functions. Since the integrals of the Bessel functions in the final results can not be further simplified, we do not list them individually.

A.4 Sakai-Sugimoto model

The model is determined by [23, 25]

$$f^2(z) = \frac{\Lambda^2(1+z^2)}{g_5^2}, \quad g^2(z) = g_5^2(1+z^2)^{1/3}, \quad z_0 = \infty. \tag{A.8}$$

In this model one only finds analytic results for the pion decay constant and the wave function ψ_0:

$$f_\pi^2 = \frac{4\Lambda^2}{\pi g_5^2}, \qquad \psi_0(z) = \frac{2}{\pi}\arctan z. \tag{A.9}$$

The quantities related to the resonances need to be calculated numerically, as done in ref. [23]. The results for the first two excitations are:

$$\begin{aligned}
m_{v^1}^2 &= 0.669\ \Lambda^2, & m_{a^1}^2 &= 1.57\ \Lambda^2, \\
a_{Vv^1} &= \frac{3.15}{g_5}, & a_{Aa^1} &= \frac{3.20}{g_5}, \\
c_{v^1} &= 0.415\ g_5, & c_{a^1} &= 0.321\ g_5, \quad d_{v^1} = 0.0875\ g_5.
\end{aligned} \tag{A.10}$$

JHEP11(2012)012

B Son-Yamamoto relation at the one-loop level

In this appendix we study the relation (4.5) between w_T and $\Pi_V - \Pi_A$, obtained by Son and Yamamoto [29], that we rewrite here:

$$w_T(Q^2) \;=\; \frac{N_C}{Q^2} \;+\; \frac{N_C}{f_\pi^2}\,(\,\Pi_V(Q^2) - \Pi_A(Q^2)), \tag{B.1}$$

at the one-loop level, as proposed in ref. [36]. This relation was derived in the large-N_C limit, i.e., for tree-level amplitudes.

At low energies, the comparison of the leading terms in the χPT expansion of the l.h.s. and r.h.s. of eq. (B.1) yields a relation between the $\mathcal{O}(p^6)$ odd-parity coupling C_{22}^W and the $\mathcal{O}(p^4)$ even-parity constant L_{10} [37], corresponding to eq. (3.27), that again we write:

$$128\pi^2 f_\pi^2 C_{22}^W \;=\; -\,4N_C L_{10}\,. \tag{B.2}$$

The possible validity of this relation (B.1) at the one-loop level was studied in ref. [36], where the AVV transition $A^3 \to \gamma\gamma^*$ was analyzed. Here A^3 refers to the t^3 generator for the axial-vector current. The Goldstone-loop contribution was computed in the two-flavor case including singlet sources, this is, in U(2), with the electric charge operator $\mathcal{Q} = t^3 + \frac{1}{6}\mathbf{1} = t^3 + \frac{1}{3}t^0$. Indeed, for $n_f = 2$ the only non-zero flavor structures come from the components $A^3 \to V^0 V^{3\,*}$ and $A^3 \to V^3 V^{0\,*}$ in the $A^3 \to \gamma\gamma^*$ transition.

The leading one-loop contribution in the χPT expansion, i.e., $\mathcal{O}(p^6)$ in w_T and $\mathcal{O}(p^4)$ in $\Pi_V - \Pi_A$, was found to also fulfill the Son-Yamamoto relation (B.1), hence it was argued that this expression might be valid beyond large N_C, at the loop level [36]. We have investigated whether the agreement between the one-loop corrections in (B.1) is also valid at higher orders in the χPT expansion. In particular, we have looked at the one-loop correction (single log) at $\mathcal{O}(p^8)$ in w_T, NLO in its χPT expansion. We have also studied the effect of considering a higher number of light quarks n_f and different flavor decay structures $A^a \to V^b V^{c\,*}$.

B.1 $VV - AA$ correlator and $A^3 \to \gamma\gamma^*$ in U(2)

Considering the $VV - AA$ correlator in the massless quark limit, we get [79]

$$\begin{aligned}\frac{N_C}{Q^2} + \frac{N_C}{f_\pi^2}(\Pi_V - \Pi_A) \;=\; & \frac{1}{f_\pi^2}\left[\,-\,4N_C L_{10} - \frac{n_f}{2}\frac{N_C}{48\pi^2}\ln\frac{-q^2}{\nu^2}\right] \\ & + \frac{q^2}{f_\pi^4}\left[8N_C C_{87} - L_9 \times \frac{n_f}{2}\frac{N_C}{12\pi^2}\ln\frac{-q^2}{\nu^2} + \mathcal{O}(N_C^0)\right] + \mathcal{O}(q^4),\end{aligned} \tag{B.3}$$

where the U(n_f) singlet components do not play here any role. We present the results for an arbitrary number of light quarks, even though we focus on the $n_f = 2$ case. We have used the $n_f = 3$ notation L_9, L_{10} and C_{87} for the $\mathcal{O}(p^4)$ and $\mathcal{O}(p^6)$ LECs, regardless of the number of light flavors.

JHEP11(2012)012

For the transition $A^3 \to \gamma\gamma^*$ with electric charge operator $\mathcal{Q} = t^3 + \frac{1}{3}t^0$, the χPT calculation up to $\mathcal{O}(p^8)$ yields:

$$w_T(Q^2) = \frac{1}{f_\pi^2}\left[128\pi^2 f_\pi^2\left(C_{22}^W - \frac{\widetilde{c}_{13}}{2}\right) - \frac{n_f}{2}\frac{N_C}{48\pi^2}\ln\frac{-q^2}{\nu^2}\right]$$
$$+\frac{q^2}{f_\pi^4}\left[K - \left(L_9 + \frac{16\pi^2 f_\pi^2}{N_C}\left(-C_{13}^W + C_{14}^W + C_{15}^W + C_{19}^W - C_{20}^W - C_{21}^W + C_{22}^W\right)\right)\right.$$
$$\left.\times\frac{n_f}{2}\frac{N_C}{24\pi^2}\ln\frac{-q^2}{\nu^2} + \mathcal{O}(N_C^0)\right] + \mathcal{O}(q^4)\,, \qquad \text{(B.4)}$$

where K represents the corresponding $\mathcal{O}(p^8)$ chiral low-energy constant. For the sake of generality, we have computed the matrix element w_T with the flavor structure specified above for a general number of light flavors, from where one can extract the expressions for the U(2) case. Notice that in addition to the single trace operator $C_{22}^W \epsilon^{\mu\nu\alpha\beta}\langle\, u_\mu\{\nabla^\gamma f_{+\,\gamma\nu}, f_{+\,\alpha\beta}\}\,\rangle$ at $\mathcal{O}(p^6)$ one also needs to take into account the contribution from a double-trace operator $\widetilde{c}_{13}\epsilon^{\mu\nu\alpha\beta}\langle\,\nabla^\gamma f_{+\,\gamma\mu}\,\rangle\langle\, f_{+\,\nu\alpha}u_\beta\,\rangle$ for $n_f \geq 3$ [46], appearing only in the U(n_f) theory. This coupling is $1/N_C$ suppressed with respect to C_{22}^W and does not appear at large N_C. However, it is essential in order to renormalize the various $A^a \to V^b V^{c\,*}$ flavor structures.

The last needed ingredient for the comparison with $\Pi_V - \Pi_A$ is the value of the $\mathcal{O}(p^6)$ odd-parity LECs which multiply the logs in w_T in terms of the $\mathcal{O}(p^4)$ even-sector couplings. For holographic models where the chiral symmetry is broken through boundary conditions [19, 24, 25, 25], we found the large-N_C relations (3.18)–(3.28) for the relevant C_k^W couplings, producing the transverse amplitude:

$$w_T(Q^2) = \frac{1}{f_\pi^2}\left[128\pi^2 f_\pi^2\left(C_{22}^W - \frac{\widetilde{c}_{13}}{2}\right) - \frac{n_f}{2}\frac{N_C}{48\pi^2}\ln\frac{-q^2}{\nu^2}\right]$$
$$+\frac{q^2}{f_\pi^4}\left[K - \left(L_9 - 2L_1\right)\times\frac{n_f}{2}\frac{N_C}{12\pi^2}\ln\frac{-q^2}{\nu^2} + \mathcal{O}(N_C^0)\right] + \mathcal{O}(q^4). \qquad \text{(B.5)}$$

The comparison of this result and $\Pi_V - \Pi_A$ in eq. (B.3) shows that there is a disagreement at $\mathcal{O}(p^8)$ in the Son-Yamamoto relation, and that the agreement at $\mathcal{O}(p^6)$ is a coincidence.

B.2 Comparison for fully non-singlet transitions $A^a \to V^b V^{c\,*}$

Indeed, the agreement found in ref. [36] at the lowest chiral order only occurs for a particular choice of the flavor structure of vector and axial-vector currents. In the case when all the three currents are U(n_f) non-singlets, one finds for the $A^a \to V^b V^{c\,*}$ transition the transverse structure function:

$$w_T(Q^2) = \frac{1}{f_\pi^2}\left[128\pi^2 f_\pi^2 C_{22}^W - \frac{n_f\, N_C}{72\pi^2}\ln\frac{-q^2}{\nu^2}\right] + \mathcal{O}(q^2)\,, \qquad \text{(B.6)}$$

to be compared to the expression which derives from the $VV - AA$ correlator,

$$\frac{N_C}{Q^2} + \frac{N_C}{f_\pi^2}\left(\Pi_V - \Pi_A\right) = \frac{1}{f_\pi^2}\left[-4N_C L_{10} - \frac{n_f\, N_C}{96\pi^2}\ln\frac{-q^2}{\nu^2}\right] + \mathcal{O}(q^2)\,, \qquad \text{(B.7)}$$

JHEP11(2012)012

for a general number of flavors n_f. The result is also valid for $n_f = 2$, although in this case the overall group factor d^{abc} in the amplitude is zero when all the a, b, c are non-singlet. One can easily see that the leading one-loop logarithms of w_T and $\Pi_V - \Pi_A$ do not match. This conclusion also comes from observing that the corresponding couplings entering at tree-level have different running [2–4, 46]:[3]

$$\frac{\mathrm{d}L_{10}}{\mathrm{d}\ln\nu^2} = -\frac{\Gamma_{10}^{(n_f)}}{32\pi^2} = \frac{n_f}{3}\frac{1}{128\pi^2}\,,$$
$$-\frac{32\pi^2 f_\pi^2}{N_C}\frac{\mathrm{d}C_{22}^W}{\mathrm{d}\ln\nu^2} = \frac{32\pi^2 f_\pi^2}{N_C}\left(\frac{\eta_{22}^{(n_f)}}{32\pi^2}\right) = \frac{n_f}{3}\frac{1}{96\pi^2}\,. \tag{B.8}$$

References

[1] S. Weinberg, *Phenomenological Lagrangians*, *Physica* **A 96** (1979) 327 [INSPIRE].

[2] J. Gasser and H. Leutwyler, *Chiral Perturbation Theory to One Loop*, *Annals Phys.* **158** (1984) 142 [INSPIRE].

[3] J. Gasser and H. Leutwyler, *Chiral Perturbation Theory: Expansions in the Mass of the Strange Quark*, *Nucl. Phys.* **B 250** (1985) 465 [INSPIRE].

[4] J. Gasser and H. Leutwyler, *Low-Energy Expansion of Meson Form-Factors*, *Nucl. Phys.* **B 250** (1985) 517 [INSPIRE].

[5] J. Bijnens, G. Colangelo and G. Ecker, *The Mesonic chiral Lagrangian of order p^6*, *JHEP* **02** (1999) 020 [hep-ph/9902437] [INSPIRE].

[6] J. Bijnens, G. Colangelo and G. Ecker, *Renormalization of chiral perturbation theory to order p^6*, *Annals Phys.* **280** (2000) 100 [hep-ph/9907333] [INSPIRE].

[7] J. Bijnens, *Chiral perturbation theory beyond one loop*, *Prog. Part. Nucl. Phys.* **58** (2007) 521 [hep-ph/0604043] [INSPIRE].

[8] O. Strandberg, *Determination of the anomalous chiral coefficients of order p^6*, hep-ph/0302064 [INSPIRE].

[9] M. Gonzalez-Alonso, A. Pich and J. Prades, *Determination of the Chiral Couplings L_{10} and C_{87} from Semileptonic τ Decays*, *Phys. Rev.* **D 78** (2008) 116012 [arXiv:0810.0760] [INSPIRE].

[10] M. Gonzalez-Alonso, A. Pich and J. Prades, *Pinched weights and Duality Violation in QCD Sum Rules: a critical analysis*, *Phys. Rev.* **D 82** (2010) 014019 [arXiv:1004.4987] [INSPIRE].

[11] K. Kampf and B. Moussallam, *Tests of the naturalness of the coupling constants in ChPT at order p^6*, *Eur. Phys. J.* **C 47** (2006) 723 [hep-ph/0604125] [INSPIRE].

[12] P. Masjuan and S. Peris, *A Rational approximation to $< VV - AA >$ and its $O(p^6)$ low-energy constant*, *Phys. Lett.* **B 663** (2008) 61 [arXiv:0801.3558] [INSPIRE].

[13] P. Masjuan and S. Peris, *A Rational approach to resonance saturation in large-N_c QCD*, *JHEP* **05** (2007) 040 [arXiv:0704.1247] [INSPIRE].

[3] After the submission of the manuscript to the arXiv we became aware that the lack of matching in SU(3) × SU(3) theory was also noticed by S. Peris and M. Knecht [113].

JHEP11(2012)012

[14] P. Masjuan, S. Peris and J. Sanz-Cillero, *Vector Meson Dominance as a first step in a systematic approximation: The Pion vector form-factor*, *Phys. Rev.* **D 78** (2008) 074028 [arXiv:0807.4893] [INSPIRE].

[15] G. Ecker, J. Gasser, A. Pich and E. de Rafael, *The Role of Resonances in Chiral Perturbation Theory*, *Nucl. Phys.* **B 321** (1989) 311 [INSPIRE].

[16] G. Ecker, J. Gasser, H. Leutwyler, A. Pich and E. de Rafael, *Chiral Lagrangians for Massive Spin 1 Fields*, *Phys. Lett.* **B 223** (1989) 425 [INSPIRE].

[17] S.-Z. Jiang, Y. Zhang, C. Li and Q. Wang, *Computation of the p^6 order chiral Lagrangian coefficients*, *Phys. Rev.* **D 81** (2010) 014001 [arXiv:0907.5229] [INSPIRE].

[18] S.-Z. Jiang and Q. Wang, *Computation of the coefficients for p^6 order anomalous chiral Lagrangian*, *Phys. Rev.* **D 81** (2010) 094037 [arXiv:1001.0315] [INSPIRE].

[19] D. Son and M. Stephanov, *QCD and dimensional deconstruction*, *Phys. Rev.* **D 69** (2004) 065020 [hep-ph/0304182] [INSPIRE].

[20] N. Arkani-Hamed, A.G. Cohen and H. Georgi, *(De)constructing dimensions*, *Phys. Rev. Lett.* **86** (2001) 4757 [hep-th/0104005] [INSPIRE].

[21] C.T. Hill, S. Pokorski and J. Wang, *Gauge invariant effective Lagrangian for Kaluza-Klein modes*, *Phys. Rev.* **D 64** (2001) 105005 [hep-th/0104035] [INSPIRE].

[22] M. Bando, T. Kugo and K. Yamawaki, *Nonlinear Realization and Hidden Local Symmetries*, *Phys. Rept.* **164** (1988) 217 [INSPIRE].

[23] T. Sakai and S. Sugimoto, *Low energy hadron physics in holographic QCD*, *Prog. Theor. Phys.* **113** (2005) 843 [hep-th/0412141] [INSPIRE].

[24] J. Hirn and V. Sanz, *Interpolating between low and high energy QCD via a $5-D$ Yang-Mills model*, *JHEP* **12** (2005) 030 [hep-ph/0507049] [INSPIRE].

[25] T. Sakai and S. Sugimoto, *More on a holographic dual of QCD*, *Prog. Theor. Phys.* **114** (2005) 1083 [hep-th/0507073] [INSPIRE].

[26] D. Becciolini, M. Redi and A. Wulzer, *AdS/QCD: The Relevance of the Geometry*, *JHEP* **01** (2010) 074 [arXiv:0906.4562] [INSPIRE].

[27] L. Da Rold and A. Pomarol, *Chiral symmetry breaking from five dimensional spaces*, *Nucl. Phys.* **B 721** (2005) 79 [hep-ph/0501218] [INSPIRE].

[28] J. Erlich, E. Katz, D.T. Son and M.A. Stephanov, *QCD and a holographic model of hadrons*, *Phys. Rev. Lett.* **95** (2005) 261602 [hep-ph/0501128] [INSPIRE].

[29] D.T. Son and N. Yamamoto, *Holography and Anomaly Matching for Resonances*, arXiv:1010.0718 [INSPIRE].

[30] A. Vainshtein, *Perturbative and nonperturbative renormalization of anomalous quark triangles*, *Phys. Lett.* **B 569** (2003) 187 [hep-ph/0212231] [INSPIRE].

[31] P. Colangelo, F. De Fazio, J. Sanz-Cillero, F. Giannuzzi and S. Nicotri, *Anomalous AV^*V vertex function in the soft-wall holographic model of QCD*, *Phys. Rev.* **D 85** (2012) 035013 [arXiv:1108.5945] [INSPIRE].

[32] I. Iatrakis and E. Kiritsis, *Vector-axial vector correlators in weak electric field and the holographic dynamics of the chiral condensate*, *JHEP* **02** (2012) 064 [arXiv:1109.1282] [INSPIRE].

JHEP11(2012)012

[33] L. Cappiello, O. Catà and G. D'Ambrosio, *Antisymmetric tensors in holographic approaches to QCD*, *Phys. Rev.* **D 82** (2010) 095008 [arXiv:1004.2497] [INSPIRE].

[34] S. Domokos, J. Harvey and A. Royston, *Completing the framework of AdS/QCD: h_1/b_1 mesons and excited ω/ρ's*, *JHEP* **05** (2011) 107 [arXiv:1101.3315] [INSPIRE].

[35] R. Alvares, C. Hoyos and A. Karch, *An improved model of vector mesons in holographic QCD*, *Phys. Rev.* **D 84** (2011) 095020 [arXiv:1108.1191] [INSPIRE].

[36] A. Gorsky, P. Kopnin, A. Krikun and A. Vainshtein, *More on the Tensor Response of the QCD Vacuum to an External Magnetic Field*, *Phys. Rev.* **D 85** (2012) 086006 [arXiv:1201.2039] [INSPIRE].

[37] M. Knecht, S. Peris and E. de Rafael, *On Anomaly Matching and Holography*, *JHEP* **10** (2011) 048 [arXiv:1101.0706] [INSPIRE].

[38] K. Kampf, *Odd sector of QCD*, *Nucl. Phys. Proc. Suppl.* **219-220** (2011) 64 [arXiv:1109.4576] [INSPIRE].

[39] D. Gomez Dumm, A. Pich and J. Portoles, *$\tau \to \pi\pi\pi\nu_\tau$ decays in the resonance effective theory*, *Phys. Rev.* **D 69** (2004) 073002 [hep-ph/0312183] [INSPIRE].

[40] D.G. Dumm, P. Roig, A. Pich and J. Portoles, *$\tau \to \pi\pi\pi\nu_\tau$ decays and the $a_1(1260)$ off-shell width revisited*, *Phys. Lett.* **B 685** (2010) 158 [arXiv:0911.4436] [INSPIRE].

[41] H.R. Grigoryan and A.V. Radyushkin, *Pion in the holographic model with 5D Yang-Mills fields*, *Phys. Rev.* **78** (2008) 115008 [arXiv:0808.1243].

[42] A. Stoffers and I. Zahed, *$\gamma^*\gamma^* \to \pi^0$ Form Factor from AdS/QCD*, *Phys. Rev.* **C 84** (2011) 025202 [arXiv:1104.2081] [INSPIRE].

[43] J. Wess and B. Zumino, *Consequences of anomalous Ward identities*, *Phys. Lett.* **B 37** (1971) 95 [INSPIRE].

[44] E. Witten, *Global Aspects of Current Algebra*, *Nucl. Phys.* **B 223** (1983) 422 [INSPIRE].

[45] E. Witten, *Current Algebra, Baryons and Quark Confinement*, *Nucl. Phys.* **B 223** (1983) 433 [INSPIRE].

[46] J. Bijnens, L. Girlanda and P. Talavera, *The Anomalous chiral Lagrangian of order p^6*, *Eur. Phys. J.* **C 23** (2002) 539 [hep-ph/0110400] [INSPIRE].

[47] T. Ebertshauser, H. Fearing and S. Scherer, *The Anomalous chiral perturbation theory meson Lagrangian to order p^6 revisited*, *Phys. Rev.* **D 65** (2002) 054033 [hep-ph/0110261] [INSPIRE].

[48] R.S. Chivukula, M. Kurachi and M. Tanabashi, *Generalized Weinberg sum rules in deconstructed QCD*, *JHEP* **06** (2004) 004 [hep-ph/0403112] [INSPIRE].

[49] G. 't Hooft, *A Planar Diagram Theory for Strong Interactions*, *Nucl. Phys.* **B 72** (1974) 461 [INSPIRE].

[50] G. 't Hooft, *A Two-Dimensional Model for Mesons*, *Nucl. Phys.* **B 75** (1974) 461 [INSPIRE].

[51] E. Witten, *Baryons in the 1/n Expansion*, *Nucl. Phys.* **B 160** (1979) 57 [INSPIRE].

[52] M. Knecht and E. de Rafael, *Patterns of spontaneous chiral symmetry breaking in the large-N_c limit of QCD - like theories*, *Phys. Lett.* **B 424** (1998) 335 [hep-ph/9712457] [INSPIRE].

JHEP11(2012)012

[53] S. Peris, M. Perrottet and E. de Rafael, *Matching long and short distances in large-N_c QCD*, *JHEP* **05** (1998) 011 [hep-ph/9805442] [INSPIRE].

[54] M. Golterman and S. Peris, *Large-N_c QCD meets Regge theory: The Example of spin one two point functions*, *JHEP* **01** (2001) 028 [hep-ph/0101098] [INSPIRE].

[55] M. Golterman and S. Peris, *On the relation between low-energy constants and resonance saturation*, *Phys. Rev.* **D 74** (2006) 096002 [hep-ph/0607152] [INSPIRE].

[56] S. Weinberg, *Precise relations between the spectra of vector and axial vector mesons*, *Phys. Rev. Lett.* **18** (1967) 507 [INSPIRE].

[57] M.A. Shifman, A. Vainshtein and V.I. Zakharov, *QCD and Resonance Physics. Sum Rules*, *Nucl. Phys.* **B 147** (1979) 385 [INSPIRE].

[58] Z. Guo, J. Sanz Cillero and H. Zheng, *Partial waves and large-N_c resonance sum rules*, *JHEP* **06** (2007) 030 [hep-ph/0701232] [INSPIRE].

[59] Z. Guo, J. Sanz-Cillero and H. Zheng, *$O(p^6)$ extension of the large-N_c partial wave dispersion relations*, *Phys. Lett.* **B 661** (2008) 342 [arXiv:0710.2163] [INSPIRE].

[60] A. Karch, E. Katz, D.T. Son and M.A. Stephanov, *Linear confinement and AdS/QCD*, *Phys. Rev.* **D 74** (2006) 015005 [hep-ph/0602229] [INSPIRE].

[61] P. Colangelo, F. De Fazio, F. Giannuzzi, F. Jugeau and S. Nicotri, *Light scalar mesons in the soft-wall model of AdS/QCD*, *Phys. Rev.* **D 78** (2008) 055009 [arXiv:0807.1054] [INSPIRE].

[62] F. Zuo, *Improved Soft-Wall model with a negative dilaton*, *Phys. Rev.* **D 82** (2010) 086011 [arXiv:0909.4240] [INSPIRE].

[63] M. Benayoun, P. David, L. DelBuono and O. Leitner, *A Global Treatment Of VMD Physics Up To The phi: I. e^+e^- Annihilations, Anomalies And Vector Meson Partial Widths*, *Eur. Phys. J.* **C 65** (2010) 211 [arXiv:0907.4047] [INSPIRE].

[64] K. Kampf and J. Novotny, *Resonance saturation in the odd-intrinsic parity sector of low-energy QCD*, *Phys. Rev.* **D 84** (2011) 014036 [arXiv:1104.3137] [INSPIRE].

[65] J. Bijnens, A. Bramon and F. Cornet, *Chiral perturbation theory for anomalous processes*, *Z. Phys.* **C 46** (1990) 599 [INSPIRE].

[66] E. Pallante and R. Petronzio, *Anomalous effective Lagrangians and vector resonance models*, *Nucl. Phys.* **B 396** (1993) 205 [INSPIRE].

[67] B. Moussallam, *Chiral sum rules for parameters of the order six Lagrangian in the W-Z sector and application to π^0, η, η' decays*, *Phys. Rev.* **D 51** (1995) 4939 [hep-ph/9407402] [INSPIRE].

[68] P. Ruiz-Femenia, A. Pich and J. Portoles, *Odd intrinsic parity processes within the resonance effective theory of QCD*, *JHEP* **07** (2003) 003 [hep-ph/0306157] [INSPIRE].

[69] R. Unterdorfer and H. Pichl, *On the Radiative Pion Decay*, *Eur. Phys. J.* **C 55** (2008) 273 [arXiv:0801.2482] [INSPIRE].

[70] P. Masjuan, *$\gamma^*\gamma \to \pi^0$ transition form factor at low-energies from a model-independent approach*, arXiv:1206.2549 [INSPIRE].

[71] V. Mateu and J. Portoles, *Form-factors in radiative pion decay*, *Eur. Phys. J.* **C 52** (2007) 325 [arXiv:0706.1039] [INSPIRE].

JHEP11(2012)012

[72] V. Cirigliano et al., *Towards a consistent estimate of the chiral low-energy constants*, *Nucl. Phys.* **B 753** (2006) 139 [hep-ph/0603205] [INSPIRE].

[73] K. Kampf, J. Novotny and J. Trnka, *On different lagrangian formalisms for vector resonances within chiral perturbation theory*, *Eur. Phys. J.* **C 50** (2007) 385 [hep-ph/0608051] [INSPIRE].

[74] M. Bando, T. Fujiwara and K. Yamawaki, *Generalized hidden local symmetry and the A1 meson*, *Prog. Theor. Phys.* **79** (1988) 1140 [INSPIRE].

[75] J. Gasser, M.A. Ivanov and M.E. Sainio, *Low-energy photon-photon collisions to two loops revisited*, *Nucl. Phys.* **B 728** (2005) 31 [hep-ph/0506265] [INSPIRE].

[76] J. Gasser, M.A. Ivanov and M.E. Sainio, *Revisiting $\gamma\gamma \to \pi^+\pi^-$ at low energies*, *Nucl. Phys.* **B 745** (2006) 84 [hep-ph/0602234] [INSPIRE].

[77] G. Colangelo, J. Gasser and H. Leutwyler, *$\pi\pi$ scattering*, *Nucl. Phys.* **B 603** (2001) 125 [hep-ph/0103088] [INSPIRE].

[78] J. Bijnens and P. Talavera, *Pion and kaon electromagnetic form-factors*, *JHEP* **03** (2002) 046 [hep-ph/0203049] [INSPIRE].

[79] G. Amoros, J. Bijnens and P. Talavera, *Two point functions at two loops in three flavor chiral perturbation theory*, *Nucl. Phys.* **B 568** (2000) 319 [hep-ph/9907264] [INSPIRE].

[80] S. Bellucci, J. Gasser and M. Sainio, *Low-energy photon-photon collisions to two loop order*, *Nucl. Phys.* **B 423** (1994) 80 [*Erratum ibid.* **B 431** (1994) 413-414] [hep-ph/9401206] [INSPIRE].

[81] M. Knecht and A. Nyffeler, *Resonance estimates of $O(p^6)$ low-energy constants and QCD short distance constraints*, *Eur. Phys. J.* **C 21** (2001) 659 [hep-ph/0106034] [INSPIRE].

[82] V. Cirigliano, G. Ecker, M. Eidemuller, A. Pich and J. Portoles, *The $< VAP >$ Green function in the resonance region*, *Phys. Lett.* **B 596** (2004) 96 [hep-ph/0404004] [INSPIRE].

[83] J. Bijnens, G. Colangelo and P. Talavera, *The Vector and scalar form-factors of the pion to two loops*, *JHEP* **05** (1998) 014 [hep-ph/9805389] [INSPIRE].

[84] J. Bijnens, G. Colangelo, G. Ecker, J. Gasser and M. Sainio, *Pion pion scattering at low-energy*, *Nucl. Phys.* **B 508** (1997) 263 [*Erratum ibid.* **B 517** (1998) 639] [hep-ph/9707291] [INSPIRE].

[85] Z.-H. Guo and J.J. Sanz-Cillero, *$\pi\pi$-scattering lengths at $O(p^6)$ revisited*, *Phys. Rev.* **D 79** (2009) 096006 [arXiv:0903.0782] [INSPIRE].

[86] A. Pich, I. Rosell and J. Sanz-Cillero, *Form-factors and current correlators: Chiral couplings $L_{10}^r(\mu)$ and $C_{87}^r(\mu)$ at NLO in $1/N_C$*, *JHEP* **07** (2008) 014 [arXiv:0803.1567] [INSPIRE].

[87] A. Pich, I. Rosell and J.J. Sanz-Cillero, *The vector form factor at the next-to-leading order in $1/N_C$: chiral couplings $L_9(\mu)$ and $C_{88}(\mu) - C_{90}(\mu)$*, *JHEP* **02** (2011) 109 [arXiv:1011.5771] [INSPIRE].

[88] J. Bijnens and P. Talavera, *$\pi \to l\nu\gamma$ form-factors at two loop*, *Nucl. Phys.* **B 489** (1997) 387 [hep-ph/9610269] [INSPIRE].

[89] J. Polchinski, *String Theory. Vol. 1: An Introduction to the Bosonic String*, Cambridge University Press, Cambridge, U.K. (1998).

[90] J. Polchinski, *String Theory. Vol 2: Superstring Theory and Beyond*, Cambridge University Press, Cambridge, U.K. (1998).

JHEP11(2012)012

[91] O. Aharony, S.S. Gubser, J.M. Maldacena, H. Ooguri and Y. Oz, *Large-N field theories, string theory and gravity*, *Phys. Rept.* **323** (2000) 183 [hep-th/9905111] [INSPIRE].

[92] K. Kampf, M. Knecht and J. Novotny, *The Dalitz decay $\pi^0 \to e^+e^-$ gamma revisited*, *Eur. Phys. J.* **C 46** (2006) 191 [hep-ph/0510021] [INSPIRE].

[93] F. Zuo and T. Huang, *Photon-to-pion transition form factor and pion distribution amplitude from holographic QCD*, *Eur. Phys. J.* **C 72** (2012) 1813 [arXiv:1105.6008] [INSPIRE].

[94] A. Radyushkin, *Shape of Pion Distribution Amplitude*, *Phys. Rev.* **D 80** (2009) 094009 [arXiv:0906.0323] [INSPIRE].

[95] M. Polyakov, *On the Pion Distribution Amplitude Shape*, *JETP Lett.* **90** (2009) 228 [arXiv:0906.0538] [INSPIRE].

[96] S. Mikhailov and N. Stefanis, *Pion transition form factor at the two-loop level vis-a-vis experimental data*, *Mod. Phys. Lett.* **A 24** (2009) 2858 [arXiv:0910.3498] [INSPIRE].

[97] X.-G. Wu and T. Huang, *An Implication on the Pion Distribution Amplitude from the Pion-Photon Transition Form Factor with the New BABAR Data*, *Phys. Rev.* **D 82** (2010) 034024 [arXiv:1005.3359] [INSPIRE].

[98] H. Roberts, C. Roberts, A. Bashir, L. Gutierrez-Guerrero and P. Tandy, *Abelian anomaly and neutral pion production*, *Phys. Rev.* **C 82** (2010) 065202 [arXiv:1009.0067] [INSPIRE].

[99] T. Pham and X. Pham, *Chiral Anomaly Effects and the BaBar Measurements of the $\gamma\gamma^* \to \pi^0$ Transition Form Factor*, *Int. J. Mod. Phys.* **A 26** (2011) 4125 [arXiv:1101.3177] [INSPIRE].

[100] S. Agaev, V. Braun, N. Offen and F. Porkert, *Light Cone Sum Rules for the $\pi^0 - \gamma^* - \gamma$ Form Factor Revisited*, *Phys. Rev.* **D 83** (2011) 054020 [arXiv:1012.4671] [INSPIRE].

[101] S.J. Brodsky, F.-G. Cao and G.F. de Teramond, *Evolved QCD predictions for the meson-photon transition form factors*, *Phys. Rev.* **D 84** (2011) 033001 [arXiv:1104.3364] [INSPIRE].

[102] S.J. Brodsky, F.-G. Cao and G.F. de Teramond, *Meson Transition Form Factors in Light-Front Holographic QCD*, *Phys. Rev.* **D 84** (2011) 075012 [arXiv:1105.3999] [INSPIRE].

[103] H. Grigoryan and A. Radyushkin, *Anomalous Form Factor of the Neutral Pion in Extended AdS/QCD Model with Chern-Simons Term*, *Phys. Rev.* **D 77** (2008) 115024 [arXiv:0803.1143] [INSPIRE].

[104] G.P. Lepage and S.J. Brodsky, *Exclusive Processes in Quantum Chromodynamics: Evolution Equations for Hadronic Wave Functions and the Form-Factors of Mesons*, *Phys. Lett.* **B 87** (1979) 359 [INSPIRE].

[105] G.P. Lepage and S.J. Brodsky, *Exclusive Processes in Perturbative Quantum Chromodynamics*, *Phys. Rev.* **D 22** (1980) 2157 [INSPIRE].

[106] S.J. Brodsky and G.P. Lepage, *Large Angle Two Photon Exclusive Channels in Quantum Chromodynamics*, *Phys. Rev.* **D 24** (1981) 1808 [INSPIRE].

[107] C. Bebek et al., *Electroproduction of single pions at low epsilon and a measurement of the pion form-factor up to $q^2 = 10$-GeV^2*, *Phys. Rev.* **D 17** (1978) 1693 [INSPIRE].

JHEP11(2012)012

[108] JEFFERSON LAB collaboration, G. Huber et al., *Charged pion form-factor between $Q^2 = 0.60$-GeV^2 and 2.45-GeV^2. II. Determination of and results for, the pion form-factor*, *Phys. Rev.* **C 78** (2008) 045203 [arXiv:0809.3052] [INSPIRE].

[109] CLEO collaboration, J. Gronberg et al., *Measurements of the meson - photon transition form-factors of light pseudoscalar mesons at large momentum transfer*, *Phys. Rev.* **D 57** (1998) 33 [hep-ex/9707031] [INSPIRE].

[110] BABAR collaboration, B. Aubert et al., *Measurement of the $\gamma\gamma^* \to \pi^0$ transition form factor*, *Phys. Rev.* **D 80** (2009) 052002 [arXiv:0905.4778] [INSPIRE].

[111] BELLE collaboration, S. Uehara et al., *Measurement of $\gamma\gamma^* \to \pi^0$ transition form factor at Belle*, arXiv:1205.3249 [INSPIRE].

[112] S.K. Domokos, H.R. Grigoryan and J.A. Harvey, *Photoproduction through Chern-Simons Term Induced Interactions in Holographic QCD*, *Phys. Rev.* **D 80** (2009) 115018 [arXiv:0905.1949] [INSPIRE].

[113] S. Peris, *The anomaly triangle and muon $g-2$*, talk given at *2012 Project X Physics Study*, Chicago, 14–23 June 2012, [https://indico.fnal.gov/conferenceDisplay.py?ovw=True&confId=5276]

JHEP11(2012)012